PERFORMANCE STUDY OF DIFFERENT TYPES OF HEAT PIPES

A Thesis Submitted in Partial Fulfillment of Requirements for the Degree of

Master of Engineering

in

Thermal Engineering

by

Shubham Srivastava

Registration no. : 802083019

Under the joint supervision of

Dr. Kundan Lal

Assistant Professor

Department of Mechanical Engineering

Dr. Sayan Sadhu

Assistant Professor

Department of Mechanical Engineering

MECHANICAL ENGINEERING DEPARTMENT

THAPAR INSTITUTE OF ENGINEERING & TECHNOLOGY, PATIALA

July 2022

DECLARATION

I, Shubham Srivastava, hereby declare that the thesis entitled " PERFORMANCE STUDY OF DIFFERENT TYPES OF HEAT PIPES " submitted to Thapar Institute of Engineering and Technology in partial fulfillment of the requirements for the award of the Master of Engineering in Thermal Engineering submitted in Mechanical Engineering Department, Thapar Institute of Engineering and Technology is a record of original and independent research work by me during the period 2020-22 under the supervision and guidance of Dr. Kundan Lal, Assistant Professor, Mechanical Engineering and Dr. Sayan Sadhu, Assistant professor, Mechanical Engineering. The work which has been done in this thesis has not been previously submitted to meet the requirements for the degree or diploma at this or any higher education institution.

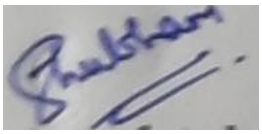

Name –Shubham Srivastava

Roll no- 802083019

Thermal Engineering (ME)

It is certified that the above statement made by the student is correct to the best of my knowledge and belief.

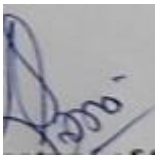

Dr.Kundan Lal

Assistant Professor (MED)

TIET, Patiala-147004

Dr.Sayan Sadhu

Assistant Professor(MED)

TIET, Patiala-147004

ACKNOWLEDGEMENT

I want to express my deep gratitude to my supervisors Dr. Kundan Lal and Dr. Sayan Sadhu for sharing with me their extremely useful suggestions, their excellent supervision, constant motivation, and encouragement through discussions have helped me in nurturing my work and preparing my manuscript through research work. I am extremely thankful to Dr. Tarun Bera (Head of the department) for his support.

I am also thankful to the Head of the central workshop for allowing me to work and use the workshop facility. I am also grateful to Mr. Charanjeet Singh and Harcharan sir instructors at the heat transfer lab for their guidance and support during my experimental work.

Name- Shubham Srivastava

Registration no- 802083019

TABLE OF CONTENTS

CONTENTS

LIST OF FIGURES

LIST OF TABLES

NOMENCLATURE

Symbol	Description	Units
g	Acceleration due to gravity	m/s^2
ß	Coefficient of thermal expansion	K^{-1}
Tc	Condenser temperature	K
Te	Evaporator temperature	K
Lc	Characteristic length	m
μ	Dynamic viscosity	Pa-s
cp	Specific heat at constant pressure	J/Kg-K
k	Thermal conductivity	W/m-K
h	Heat transfer coefficient	W/m^2K
Q	Heat input	W
ρ	Density of air	kg/m^3
V	Velocity of air	m/s
D	Diameter of the specimen(under testing)	m
A	convective heat transfer area	m^2
Tw	Wall temperature	K
Tb	the average temperature of the air entering and leaving	K
Tf	Film temperature	K
Ta	Ambient temperature	K

Symbol	Non- dimensionless number
Gr	Grashoff number
Pr	Prandtl number
Nu	Nusselt number
Ra	Rayleigh number
Re	Reynolds number

SUBSCRIPTS

c	Condenser
e	Evaporator
th	Theoretical
in	Input
exp	Experimental
w	Wall
b	Average bulk temperature
f	Film
a	Ambient

ABSTRACT

Despite the abundant studies on heat pipes over the last fifty years, the development of analytical tools for the design of heat pipes remains challenging, even for conventional technologies. As a result, heat pipes are still the object of more than 250 scientific articles a year. A brief overview of the heat pipe history is given and the different applications are presented. The different types of heat pipes are tested in different conditions that are under forced and free convection to identify the performance of different kinds of heat pipes. In natural convection conditions, heat input is increased from 20 to 35V and surface temperature is observed then by using correlations we try to find out h (heat transfer coefficient), and a comparison is made between analytical and experimental h (heat transfer coefficient). Similarly in the case of forced convection by varying velocity between 9m/s to 30m/s and keeping heat input constant that is 20V we try to find out heat transfer coefficient experimentally and then compare that heat transfer coefficient with the analytical heat transfer coefficient which we obtain using correlations.

Keywords: heat pipes, natural convection, forced convection, heat transfer coefficient, aluminum plugs, finned aluminum rods, finned heat pipes.

CHAPTER 1: INTRODUCTION

Heat pipes are passive devices that transport great heat amounts by using latent heat of an inner working fluid. It has many applications due to its great demand in the market and technology. The heat transfer in heat pipes happens at almost isothermal conditions, with a minimal temperature change as a driving force. Due to their high conductance, a heat pipe can transport heat efficiently from a source to a remote sink. A heat pipe consists of three main components: evaporator, adiabatic section, and condenser. The input of the heat occurs through the evaporator part, which evaporates the working fluid inside the heat pipe, after this process the flow of vapor occurs along the adiabatic section towards the condenser section. During the process of condensation, the fluid goes back to the evaporator section, completing the cycle. The return of the fluid can happen by capillarity through an internal wick, or by gravity. In wickless heat pipes or what we call a thermosyphon the return of fluid takes place through gravity.

A heat pipe is a device that is well known because of its characteristics like high heat transfer and its ability to extract heat with minimum loss. It has various applications with the advancement in technology the machinery which is used nowadays require heat pipes for heat recovery and heat extraction. The forces which are involved in heat pipes are capillary and gravitational forces which play an important role in determining the efficiency of heat pipes because at different inclinations the resultant of these forces vary accordingly. It offers many advantages like it has compact size and can transfer heat over the desired range with minimum temperature which helps in reducing the load on the equipment.

The heat pipe, the term was coined by Grover however he was not the first person, he followed the work of ‘Gaugler’ who introduced the wick's concept of the heat pipe in 1944 due to which later term ‘heat pipe’ came into depiction [Solar thermal systems components and applications, 2012].

There are distinct types of wick systems to improve the performance of capillary force in heat pipes, such as; screen mesh, sintered metal, axial grooves, open annulus, or artery wick in wicked heat pipes. The wick selection depends on the heat pipe working condition and aim, to

get the best wick design. During the initial phase of selecting a heat pipe wick, three important parameters must be taken into account: minimum capillary radius, permeability, and effective thermal conductivity. For extremely large capillary pressure, a minor capillary radius is required. The permeability computes the axial liquid flow; the higher the permeability is, the

lesser liquid pressure drop across the wick will be. Big values of effective thermal conductivity mean a small temperature drop in the wick. Heat pipes and thermosyphon are somewhat the same kinds of devices but the key difference is that heat pipes can work against the gravitational forces whereas thermosyphon cannot work against it because it does not have the wick structure which can condensate the liquid back to the evaporator section. An experimental study of different kinds of heat pipes under free and forced convection conditions has been carried out, various input parameters have been varied to understand the behavior of different specimens and the heat transfer coefficient has been evaluated through analytical and experimental methods and a comparison is made between them.

1.1 Construction of heat Pipe

The three basic sections of a heat pipe are shown in Fig. 1. Heat pipes generally have three components; container, working fluid, and wick.

1.1.1 The container**:** The function of the container is to isolate the working fluid from the surroundings. It has should have the following characteristic it should be leakproof, maintain the pressure differential across its walls and enable the transfer of heat to take place from and into the working fluid. To avoid the diffusion of vapor the material selected should be nonporous. To ensure minimum temperature drop, between the heat source and wick thermal conductivity should be high.

The selection of the container material depends on many factors these are as follows;

1. Compatibility
2. Strength-to-weight ratio
3. Thermal conductivity
4. Ease of fabrication, including welding machinability and ductility
5. Porosity
6. Wettability

Generally, in heat pipes the container used is a vacuum-sealed hollow container which consists of three parts that are the evaporator section, the adiabatic section, and the condenser section, there are many materials used in a container like aluminum, copper, and stainless steel but generally, copper is used.

High conductivity material is used for the container. During the working of the heat pipe there comes a stage where the liquid is left only in a small portion that is the majority portion occupied by the vapor. The container should be such that it has more strength and less weight. In some applications where there was high heat rejection required, fins were employed on the condenser as we know fins are used to increase the heat transfer rate by increasing the surface area.

1.1.2 Working fluid

The main characteristic of the working fluid on which its selection depends is the operating vapor temperature range. Within an approximate temperature band, many possible working fluids may exist, so the selection of working fluid also depends on other variety of characteristics that must be examined to determine the utmost adequate of these fluids for application measured. The desirable characteristic of the working fluid are;

1. Compatibility (with wick and wall material.)
2. Good thermal stability.
3. Wettability (of wick and wall materials).
4. Vapour pressure is not extremely excessive or little over the operating temperature range.
5. High latent heat.
6. High thermal conductivity.
7. Low liquid and vapor viscosities.
8. High surface tension
9. Adequate freezing or pour point.

There are various limitations to heat flow occurring within the heat pipe such as viscous, sonic entrainment, and nucleate boiling levels and the selection of working fluid depends on these limitations. A high value of surface tension is desirable to enable the heat pipe to operate against gravity and generate a high capillary driving force. In some cases, a merit number is also very useful to compare two different working fluids. Merit number is directly proportional

to surface tension and latent heat of vaporization and liquid density is inversely proportional to liquid viscosity. Merit number is always useful for working fluids. In working fluid, high surface tension is required, it is also necessary for the working fluid to wet the wick and the container material, that is, the contact angle should be zero or very small. To avoid high vapor velocities, the vapor pressure over the operating temperature range must be high which tends to set up a large temperature gradient and cause flow instabilities.

In the case of heat pipes when we want to transfer large amounts of heat with minimum fluid flow, high latent heat of vaporization is required and hence maintaining low-pressure drops within the heat pipe. To minimize the radial temperature gradient and to reduce the possibility of nucleate boiling at the wick or wall surface the thermal conductivity of the working fluid should preferably be high. The opposition to fluid flow will be lessened by choosing fluids with low values of vapor and liquid viscosities.

1.1.3 Wick

The wick is a porous kind of structure made of materials such as steel, aluminum, nickel, or copper in various ranges of pore sizes. Wick is produced using metal foams, and more particularly made from a type of soft cloth made from wool, which is more frequently used. The main purpose of the wick structure in the heat pipes is that it is used to transfer the condensed liquid back to the evaporator as shown in Fig.1. The function of the wick is that it should produce capillary pressure and it should pass the liquid back into the evaporator at the desired rate. There are many types of wick structures used that offer a different magnitude of capillary forces to bring liquid back into the evaporator section, the most common type of wick structure used is a wrapped screen. The maximum capillary head generated by wick increase with a decrease in pore size. The wick permeability increases with an increase in pore size. The capability of the heat pipe to transport heat is raised by increasing the wick thickness. The overall thermal resistance at the evaporator also depends on the thermal conductivity of the working fluid in the wick. The most common types of wicks used are – sintered powder, groove tube, and screen mesh.

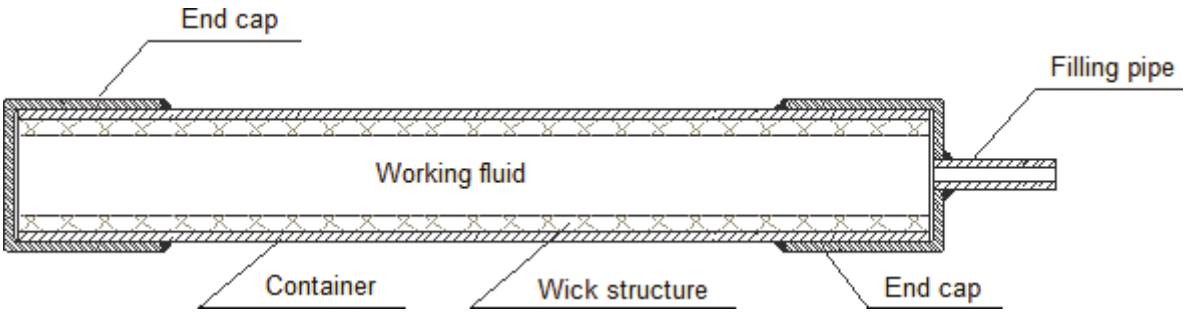

Fig. 1.1: Construction of heat pipe (Patrick Nemec, 2018)

1.2 Working of the heat pipe

The container has a liquid inside it, under its pressure, which enters the pores of the capillary material, which wets all internal surfaces and when heat input is given at any point along the surface of the heat pipe it causes the liquid at that point to boil and enter a vapor state. Once that occurs, the liquid picks up the latent heat of vaporization. The gas, which then has a higher pressure, moves inside the sealed container to the colder location where it condenses. The vapor condensation happens when the temperature is lower than that of the evaporator. A constant temperature is maintained along the length of the heat pipe due to high thermal conductance. When the condensate is returned from the condenser end to the evaporator end through capillary forces the cycle is completed. The thermal conductivity of heat pipes is very high, almost thousand times that of copper. Its “axial power rating (APC)” defines the heat transfer or heat transport capacity of a heat pipe. It shows the energy which is moving axially along the pipe. The larger the heat pipe diameter, the greater the APR. Likewise, the longer the heat pipe lesser the APR. Heat pipes can be manufactured in almost any size and shape. This has also been explained in Fig. 2.

The heat pipes system is well proven in many areas and applications the most prominent of them is aerospace applications.

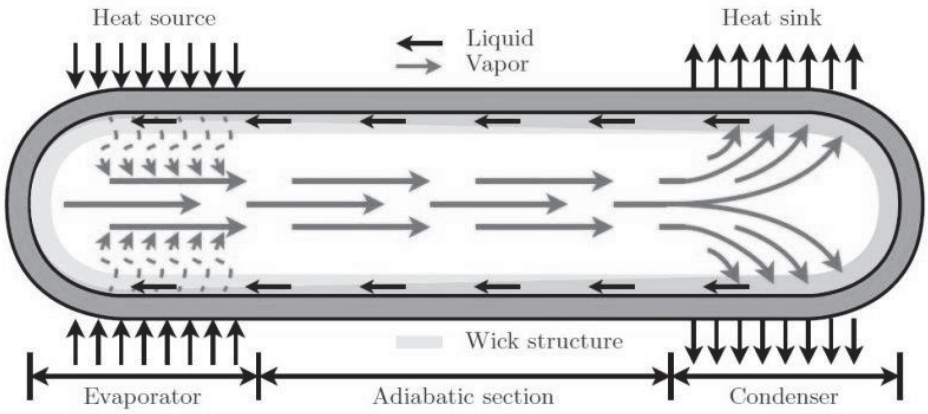

Fig. 1.2: Working principle of the heat pipe (David Gonzalez Pena,2019)

1.3 Types of heat pipes

There are different types of heat pipes that are used in various applications as per the requirement. Some of them have been explained below;

1.3.1 Oscillating heat pipes

1.3.2 Loop heat pipes

1.3.3 Thermosyphons

1.3.1 Oscillating heat pipes

These types of heat pipes (OHPs) work on the principle of pressure and temperature changes which occurs during the phase change of the working fluid and a pulsating motion of liquid slug and vapor bubbles between the evaporator and the condenser is created due to this reason as shown in Fig 3. The liquid and vapor flow are conducted without the need for the wick in OHPs. Oscillating heat pipes were invented in the early 90s and continuous efforts have been made to implement the technology in the field of cryogenics. The first loop heat pipe working at liquid nitrogen temperatures was presented in 1991 and demonstrated in 1998 that loop heat pipes can be made to function at any cryogenic temperature down to 4K.

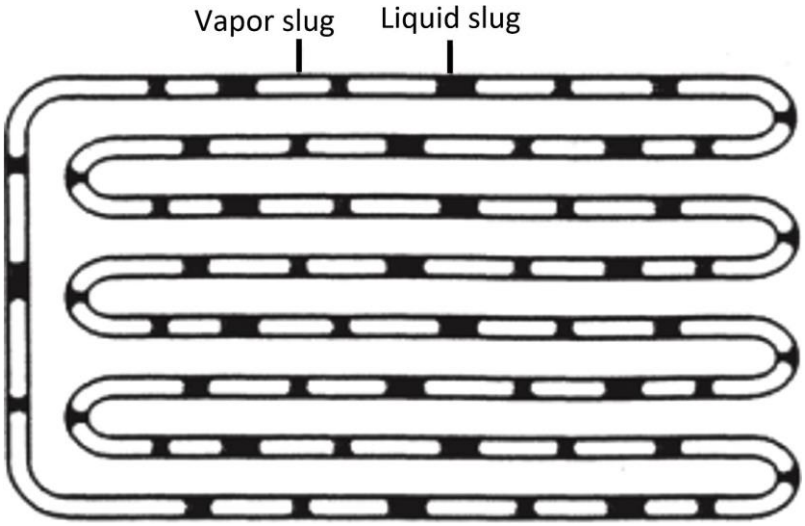

Fig. 1.3: Oscillating heat pipes (A. Chauhan, 2017)

1.3.2 Loop heat pipes

The high heat transfer capacity, the ability to operate at any different angles, the ability to remove heat from several spatially separated sources, the apparent liquid/vapor transportation lines, and most important the governability of loop heat pipes (LHPs) separate them as attractive two-phase heat transfer devices. During the operation of an LHP system, some part of the condenser is filled with vapor, which transmits the heat output, and the remaining part is filled with liquid. At the same time, the compensation chamber is partially filled with liquid and saturated vapor, which allows the volumetric proportion to change according to the heat input. During the initial phase, of the LHP operation, as the heat input increases, the mass flow rate is increased and thus more liquid is pushed to the compensation chamber but as the process continues the number of vapor increases, which decreases the sub-cooling of the returned condensate. In the latter case, when the condenser is fully used and the liquid displaced is entirely located in the compensation chamber, the LHP will function at constant conductance.

To establish the ideal performance of a cryogenic LHP (CLHP) system, the working fluid inventory has to occupy the compensation chamber at a proper level. However, for a given reservoir volume, the working fluid inventory executes a limitation on the heat transfer capability of a CLHP when the inventory is less or greater than the ideal value, as the operating

temperature and pressure will increase very quickly resulting in the reduction of surface tension and capillary pressure. Moreover, other difficulties with CLHPs are that to start up a CLHP the working fluid must be first cooled below its critical temperature until it condenses and saturates the evaporator wick.

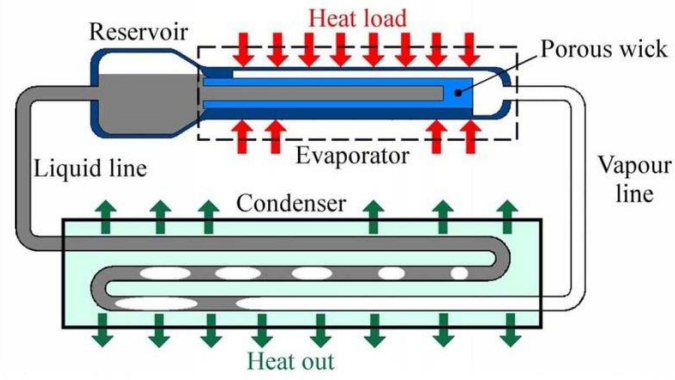

Fig. 1.4: Loop heat pipes (Laetitia Mottet, 2014)

1.3.3 Thermosyphon

The thermosyphon is a gravity-assisted heat pipe, in which the condensate returns to the evaporator due to gravitational forces as the evaporator and the condenser are positioned with an inclination angle between them. The best performance of the thermosyphons is achieved when they are oriented vertically, as the distance between their top and bottom is sufficiently large to set up the necessary natural convection flow. The research work which has been done on cryogenic thermosyphons is quite limited compared to other categories of low and ultra-low applications heat pipes.

Some researchers focused their studies on identifying the heat transfer characteristics of cryogenic thermosyphons. The most popular devices are those in which there is copper as the casing material and nitrogen, helium, or argon is the working fluids. The temperatures achieved were between 4 and 145 K(270 to 130 °C). Bolozdynya examined the heat transfer capabilities of a cryogenic copper thermosyphon filled with nitrogen as the working fluid for a filling ratio (FR) of 3.2% and 6.5%. To provide the cooling effect, the condenser of the system was absorbed into a free boiling liquid nitrogen pool. The system operated between the temperatures of 80 to 120 K (-193°C to 153°C) [B. Delpech, 2017].

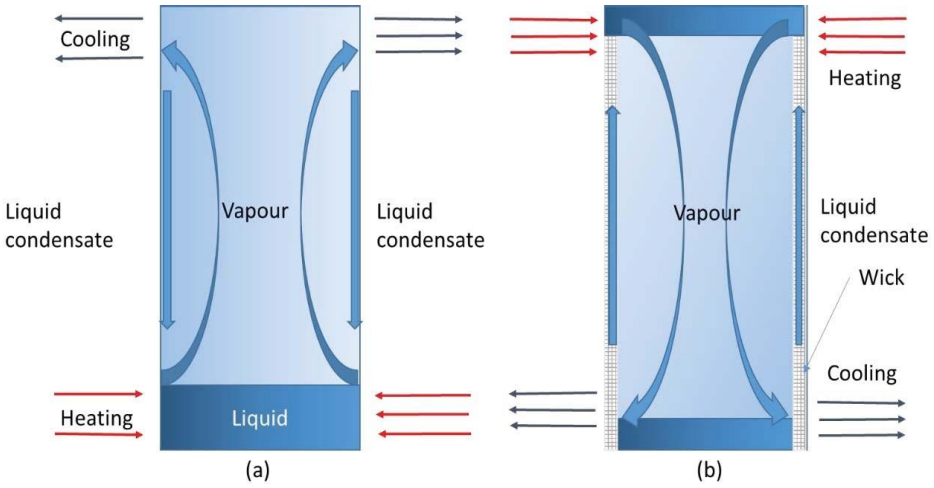

Fig. 1.5: (a) Thermosyphons (b) Heat pipes (Ivan Alonso De Miguel, 2019)

Table 1: Heat pipes with different structures and operating conditions(Rebecca Oday,2022)

Working fluid	Operating temperature (°C)	Wick design	Wall material	Axial heat transport (W)
Methane	-140	Circumferential mesh	Stainless steel	12
Water	100	Axial grooves	Copper with a rectangular cross-section	70
Sodium	430-790	Circumferential stainless-steel screen	Stainless steel	1309

1.4 Limitations in heat pipes

The heat pipe has to operate inside the dome region as shown in Fig. 6. For the heat pipe to function well the maximum capillary pressure should always be more than the total pressure drop inside the pipe. This pressure drop consists of the following three components;

1-The pressure: drop to bring the liquid from the condenser back to the evaporator.

2-The pressure: drop so that the vapor from the evaporator can reach the condenser.

3-The pressure: drop due to gravity which can be zero, negative, or positive depending on the orientation of the heat pipe.

$$\Delta P_c(max)=\Delta P_l + \Delta P_v + \Delta P_g \quad (1)$$

The heat pipe will not function properly if the above equation is not satisfied.

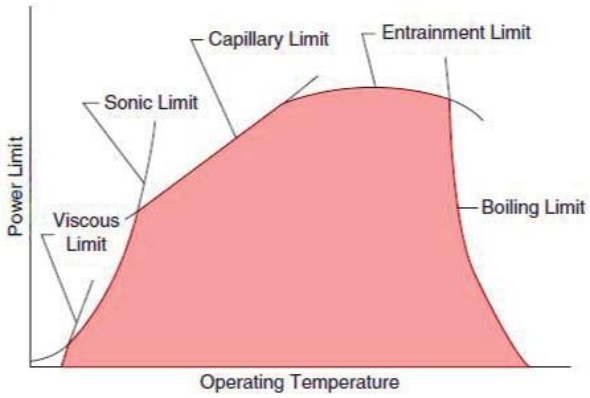

Fig. 1.6: Limitations in heat pipe (Cristina Alonso,2019)

1.5 Applications of heat Pipes

There are many applications of heat pipes like;

1.5.1 Solar application
1.5.2 Geothermal application
1.5.3 Automotive industry
1.5.4 Nuclear

1.5.1 Solar applications

The usage of heat pipes in a solar thermal collector is the most common application of high-temperature thermosyphons. The thermal absorption of a solar thermal collector is usually completed in a parabolic or flat heat pipe application. To upsurge thermal conductivity within thermosyphon-based systems, metallic nanoparticles have been added due to their high thermal

conductivity. Ghasemi and Ranjbar modeled the execution of nanoparticles in a parabolic thermosyphon [H.Jouraha,2017]. Both Al_2O_3 mixture and water were simulated and compared. As previously modeled, the application of Al_2O_3 had a meaningfully increased thermal conductivity compared to a simple water solution commonly used in water-based solar thermal collectors.

Both the modeling of solar thermal collectors and a nanofluid working fluid are relatively new technologies and their amalgamation is yet to be simulated. An inflated level of precise experimental work exists around solar thermal collectors such as flat heat pipes compared to conventional water collectors, but these are yet to be simulated in a solar thermal application. Solar thermal heat pipe applications simulations have not been done yet, as the heat pipe is usually assumed to be a flat heat pipe. As this is a relatively new technology, simulations in the part are still very inadequate.

1.5.2 Geothermal application

The application of heat pipes in geothermal applications allows the extraction of heat from a ground source to provide an alternative renewable technology. The employment of heat pumps permits the thermal system to act as a heat sink in warmer climates and a heat source in cooler months. Congledo *et al.* (year) modeled three dissimilar geometric ground heat exchangers, and a series of simulations were conducted to examine the thermal properties in both winter and summer applications [A. Chauhan,2017]. Zhang *et al.* (2016) considered the thermal characteristics of a thermosyphon when executed into a permafrost region [Wrobel, 2017].

Classically, regions of permafrost are highly delicate to climate change, thus varying the thermal performance of the implemented thermosyphon. Modeling in permafrost areas had only been directed through numerical means, allowing prolonged transient simulation but without identifying thaw regions. CFD models allow the simulation of identical transient conditions but will classify thaw zones and areas of sub-soil pool formations. Mu et al. executed a heat pipe system within permafrost regions to prevent thawing. The investigation had only been conducted through theoretical models and physical experimentation. Both phenomena had been physically experimented with but had not been simulated through a CFD model.

1.5.3. Automotive industry

The application of heat pipes has an increasing application with hybrid vehicles, in particular the addition of flexible heat pipes in a battery cooling unit. The research around flexible heat pipes was vastly noted within computer cooling technologies. The hybrid vehicle technology faces many issues regarding heat pipes, with the main apprehension surrounding the problems to reach the thermal requirements under different operation conditions.

Likewise, to the designs detected in the computer cooling industry, the addition of more complex pipes and wick structures could significantly increase the operation. Complex heat pipes used for cooling a CPU have been recognized to be more operative, as, in theory, the adaption of CPU-style heat pipes seems like a good idea but the scalability of such a technology was the main limiting factor in conjunction with other variables such load conditions. The capacity of the battery under dissimilar load conditions with regards to the applicability is dependent on the application and usage of the battery unit. The growth of hybrid systems using heat pipes using a flexible geometry, in combination with other technologies such as oscillations, could prove to be operative under multiple load conditions.

1.5.4 Nuclear sector

The heat pipe includes a neutron absorber core bounded in a wick structure. The modeling of hybrid heat pipe structures includes both a homogeneous and a reactive model, due to the radioactive materials at the same time within the metal cask. The area which surrounds the wicked core occurs as a homogeneous model, whereas the wicked core comprises a permeable surface that allows cooling. Pavlo et al. modeled the execution of a thermosyphon system in a cold neuron source system. Simulations of such a system were carried out by modeling an external hydrogen flow by using a RANS turbulence model, but an internal multiphase model had not been applied. The modeling of nuclear heat pipes is very inadequate, with the mainstream simulation being intensive on single pipe structures. The modeling of nuclear reactions is a compound procedure with certain limitations such as reaction rates, decay, and the material properties of the radioactive matter.

CHAPTER 2: LITERATURE REVIEW

In the study undertaken, many research papers were referred to as understanding the concept and working of different types of heat pipes. However, the relevant papers have been discussed over here as the part of literature review.

Teng *et al.* (2010) presented the study of enhancement of thermal efficiency of heat pipe charged with nanofluid. He considered alumina nanofluid which was produced by a direct synthesis method with three different concentrations (0.5, 1.0, and 3.0 wt. %). The nanofluid was dispersed many times with the help of an ultrasonic vibrator and electromagnetic agitator and suspension were statically placed for 1 month to ensure good suspension. He took a straight copper pipe with 8 mm inner diameter and 600 mm length and investigated the effect of different charged amounts and tilt angles. His investigation revealed that the performance of the heat pipe was optimized at 1.0 wt. % concentration of nanofluid and increased efficiency of 16.8% compared to the base fluid.

Mousa (2011) studied the effect of nanofluid concentration on the performance of a heat pipe. The author used pure water and Al_2O_3-water-based nanofluid as working fluids. An experimental setup was made to study the heat pipe performance in varying operating conditions. Theeffect of the fraction of nanoparticles in the base fluid by volume, filling ratio, and the input heat fluxon the thermal resistance of the heat pipe was studied. The total thermal resistance of the heat pipe for pure water and Al_2O_3-water-based nanofluid was also predicted. The author observed that the thermal resistance decreases with increasing Al_2O_3-water-based nanofluid compared to that of pure water.

Riehl *et al.* (2011) investigated water-copper nanofluid application in an open-loop pulsating heat pipe. They used an open loop pulsating heat pipe with water-copper nanofluid by using the addition of 5% by mass of copper nanoparticles. Improvements in the overall device's operation were noticed by the author when using the nanofluid with lower temperatures. In their work, more bubbles were formed, so more intense pulsations were observed during the PHP operation, which resulted in more presence of vapor in the channels. Hence higher thermal conductance was seen when compared to the pulsating heat pipe operation with pure water as the working fluid.

Solomon *et al.* (2020) experimented to study the effect of coated wick on the performance of heat pipe by taking a wick of screen type (100 mesh/inch) with and without deposition of the nanoparticles.80-90nm copper nanoparticles were coated over the wicksurface by a simple

immersion technique and followed by drying and the heat pipe was tested at three different heat fluxes. The result showed that with coated heat pipe wall temperature decreases as compared to uncoated heat pipe further it revealed that thermal resistance of the evaporator section decreased and that of condenser increased but overall thermal resistance was lower than that of conventional and it decreases with increased heat input. He observed a 40% reduction in thermal resistance and a 40% increase in heat transfer coefficient.

Hung *et al.* (2017) carried out his examination with alumina nanofluid which was formed by direct synthesis using dispersant cation chitosan as base fluid. He took three variants ofthe nanofluid 0.5, 1.0, and 3.0 by weight percent in the heat pipe, a straight copper tube having a 9.52mm outer diameter and diverse lengths of the heat pipe (0.3 m, 0.45 m, and 0.6 m) dissimilar charged volume ratio of base fluid 20%, 40%, 60%, 80%, respectively, the effect of tilt angle 10˚, 40˚, 70˚ and 90˚, different heat input (20 W, 30 W, and 40 W) and studied the effect of these variants on the effective thermal conductivity of the heat pipe to know the thermal performance of heat pipe. Results demonstrated that every parameter affected the performanceof the heat pipe.

Peyghambarzadeh *et al.* (2013) functioned on the thermal performance of different working fluids in a dual diameter circular heat pipe. The performance of a circular heat pipe of 40 cm in length was experimentally checked. The heat pipe had two diameters, broader in an evaporator and narrower in adiabatic and condenser regions. Three different working fluids water, methanol, and ethanol were introduced separately inside the heat pipe. The evaporator is subjected to low heat flux values. While in a condenser, the Author used a constant temperaturewater bath at 15 ˚C, 25 ˚C, and 35 ˚C. Compared to methanol, results obtained showed that higher heat transfer coefficients were obtained for water and ethanol. Also, with an increase in heat flux, the heat transfer coefficient at the evaporator rises. Using methanol, a reduction in heat transfer coefficient is observed at high heat fluxes which are probably due to the surface dry-out effect. Increasing the orientation decreased the heat pipe thermal resistance.

Xue *et al.* (2020) performed experiments to study the performance of a pulsating closed-loop heat pipe with a 50% filling ratio ammonia working fluid. The heat pipe was made out of quartz glass with six turns. The inner and outer diameters were 2 mm and 6 mm, respectively.The movement of flow could be perceived by visual study only, but the author had to perform 4 case tests to decide the effects of heat pipe orientations on its performance. The results showed that, at any arbitrary inclination angle, the ammonia circulation was very

smooth and easy. Thermal resistance as low as 0.02 K/W was attained which reflects the efficient and fast performance of the heat pipe. Also, thermal resistance was found to be inversely proportional to the inclination angle. The ammonia closed-loop heat pipe at horizontal 0 degrees position, when put to low input load, was very simple to start, but the flow of working fluid in such case was slow.

Hassan *et al.* (2012) studied the effect of alumina nanoparticles organized by a two-step method onthe performance of heat pipe taking the nanofluid (1 and 3% wt.) of 20-50 nm diameter sizein deionized water and the result was compared with heat pipe having deionized water only. For this, they took a heat pipe of 10 mm inner diameter, 200 mm brass tube with 50 mm long evaporator and 50 mm long condenser and exhibited that with nanofluid wall temperature was decreased and the difference between the condenser temperature and evaporator temperature was also reduced. Further, he said that the increase in the thermal diffusivity of the nanofluid was 10%. His investigation discovered the variation of viscosity of nanofluid as compared to deionized water and also showed that the evaporator temperature was lesser than that of deionized water with increasing heat input.

Wei Wu *et al.* (2018) established a novel solar water heating system (SWHS), which has the capability of dropping the consequence of solar radiation intensity fluctuations, been made up by using phase change materials (PCM) for thermal energy storage and introduced oscillating heat pipe (OHP) for performance enhancement. Various working modes can be selected according to the solar radiation intensity in different seasons and different climate conditions. A test rig was developed for the performance measurement of the system. The full-year measurement in all kinds of environmental conditions had been carried out for a couple of consecutive years, in Nanjing city of China. The performance of a system, such as collecting efficiency (CE), average collecting efficiency (ACE), coefficient of performance (COP), and exit water temperature (EWT), had been measured and compared between the systems with and without PCM. Under alike operation conditions, the system with PCM is demonstrated to have much-improved performance. In the daytime, CE variation with PCM is over 30% less than that without PCM. At summer night, EWT with PCM can keep over 50 °C, while EWT without PCM has an obvious decrease. At winter night, COP with PCM is over 3.0 which can make EWT reach 50 °C in a much shorter time than that without PCM. The system presented proved to be effective and useful in the application of solar energy.

Jouhara *et al.* (2016) built a heat exchanger in which the charging channel was built by stainless steel heat pipes. The heat pipes transported heat from a steam flow then cold water

flowed through a stainless steel coil injected into the latent TES tank too. The experiments showed the possibility of this concept for waste heating recovery. Of all the experimental studies considered, only one was focused on hybrid, heat pipes, and PCM, a system for refrigeration.

Hu *et al.* (2018) investigate the effect of inclination angle on two types of heat pipes: Photovoltaic/thermal (PV/T) wickless heat pipe and PV/T wire-meshed heat pipe. They found that the inclination angle has an important effect on wickless heat pipes, whereas the effect of the inclination angle was irrelevant for the mesh heat pipes. This is due to the capillary force produced by the mesh that dominates liquid cycling inside the heat pipe.

Teng *et al.* (2018) experimentally investigated the enhancement of heat pipe performance utilizing two kinds of working fluids: DI water and Al2O3-water nanofluids. Many parameters were observed in their study including charge ratio, concentrations of nanoparticles, and the tilt angle. Three different concentrations were used: 0.5, 1.0, and 2.0 wt%. Heat pipe thermal efficiency increased by 16.8% using 1.0 wt% Al2O3-water over the DI water heat pipe. Both heat pipes showed performance improvements as the inclination angle increased up to 60, above which, heat pipe performance started to drop.

Min *et al.* (2018) demonstrated the effectiveness of copper surface treatments on a finned heat pipe experimentally. The hydrophilic coatings were synthesized by immersing the heat pipe in a solution of sodium hydroxide (NaOH) and potassium persulphate (K2S2O8). This experiment proved that these methods of treatment efficiently promoted the surface wettability so that the cooling capacity of the treated heat pipe was increased significantly compared to the untreated one.

Jawad *et al*. (2020) has projected the thermal behavior of wickless heat pipes with a commercial CFD code. A 2-D CFD model of the wickless heat pipe using ANSYS Fluent was established using a user-defined function. Temperature plots and thermal resistance along the wickless heat pipe have been plotted under various working conditions regarding filling ratios, orientation angles, and heat addition. The author authenticates results with experiments. It had observed thermal resistance along the wickless heat pipe was reduced by increasing the heat addition. And the filling ratios on the average temperature of the evaporator wall at comparatively high heat added are clearer compared with minor heat addition. The author highlighted various patterns and heat transfer at different functioning parameters using a software package to increase understanding of the phenomenon.

Jemni *et al.* (2021) hotspots have become a widespread problem in electronic chips. Thermal management of hotspots is challenging because of their unstable three-dimensional circulation, e.g., in high-speed microprocessors chips with regularly changing loads and high-density power electronics with quickly evolving output demands. In this literature, three-dimensional flat plate heat pipes with many heat sources are investigated numerically using CFD software. Using copper foam as a wick structure is considered, and the result of positions of hotspot and heat flux on heat pipe performance is assessed. It is observed that copper metal foam can be used as another wick for flat plate heat pipe Contours made taking into consideration that the hot spot 17 position affects different heat flux. It was observed that top hot spot positions, incredibly close to the wall, are dangerous points where dry-out can occur because Hot spot dimensions and their distances and effective pore radius had affected heat pipe operation very much.

Hao *et al.* (2018) showed an overall enhancement of heat pipe performance using CuO layer coating. For a given charging ratio, the heat pipe with nano-engineered evaporator sections can also effectively prevent flooding owing to the coating's superior capillarity, which evenly distributes liquid to the entire evaporator surface areas.

Chan *et al.* (2017) investigated the different types of wicks alongside different types of heat pipes. The study itself was mainly based on experimental, with slight discussion around validation methods. The absence of validation within the review paper does not fully recognize the ideal conditions for certain wick and heat pipe types. The paper suggests the study of different shapes, but likewise, the experimentation is rare, but the initial result shows potential for expansion. The study classifies the most current application around oscillating and rotating heat pipes, which can be useful in multiple sectors ranging from low-temperature heat pipes and engine coolant systems. The complete findings present infinite possibilities but the lack of validation around these topics poses a problem, particularly with the growth of hybrid technology.

Bolozdynya *et al.* (2020) examined the heat transfer capabilities of a cryogenic copper thermosyphon filled with nitrogen as the working fluid for a filling ratio (FR) of 3.2% and 6.5%. To provide the cooling effect, the condenser of the system was immersed in a free boiling liquid nitrogen pool. The system operated between the temperatures of 80 to 120 K (-193 C to 153 C), while its heat transfer limit was 100 W.

Moravia *et al.* (2018) investigated the thermal performance of heat pipes by taking aluminum

oxide nanoparticles of diameter 35nm. He took a heat pipe made of copper with different lengths which has sintered wick structure and a 90˚ curve between the evaporator and condenser section. Tested concentrations of nanofluids were 0%, 1%, and 3% by weight. He compared the result obtained with a heat pipe charged with pure water. His results showed that an increase in heat input increases the wall temperature, the wall temperature of the heat pipe with nanofluid was less as compared to the heat pipe charged with the pure water wall temperature decreased with higher nanoparticle concentration also with increased nanoparticle concentration, the temperature difference decreases. The result showed that the thermal resistance of a heat pipe with nanofluid was lower than that of a water heat pipe.

Kumar *et al*. (2015) examined that mini cylinder-shaped powder metal sintered wick heat pipe (sintered heat pipe) has inflated thermal efficiency for high heat flux electronics device cooling. In this literature, heat pipes with multiple different Wick geometries of dimensions 0.5mm,0.75mm, and 1mm along with Sintered, V-Groove, Screen Groove wick shapes are selected, Silica is used as a Heat pipe material, and nickel alloy nisi (nickel + silicon) is utilized as wicking medium. Aqueous Methanol, water, and Methanol are selected as the working fluids. The author performed simulations on the CFD software package at various temperature gradients and heat transfer coefficients having multiple wicks, wick shapes, and different working fluids.

Saeed Tiari *et al*. (2017) studied the charging and discharging processes of a latent heat thermal energy storage system assisted by a heat pipe network experimentally. Rubitherm RT55 was chosen as the phase change material (PCM) and was bounded within a vertical cylindrical container. A network of simulated heat pipes was enclosed within the PCM to improve the heat transfer. The heat pipe array contained a central heat pipe with an array of secondary heat pipes. The primary heat pipe carries forward the thermal energy from the heat source to the heat sink while the secondary heat pipes transport the extra thermal energy into the phase change material during the charging process or regain it from the phase change material during the discharging process.

The heat pipe network was made simple by engaging an arrangement of copper and acrylic pipes. Water was used as the heat transport fluid, which was circulated through the pipe network with a relatively high velocity to decrease the temperature drop, like what happens inside a real heat pipe.

Manimaran *et al.*(2018) conducted a series of experiments on copper heat pipes using deionized (DI) water as a working fluid with four different inclination angles. The results showed that the thermal resistance and efficiency of a heat pipe are exaggerated directly by the charging ratio. They displayed that the thermal resistance diminished as the charging ratio increased up to 75% of the evaporator section volume of the heat pipe. Above this span, the thermal resistance begins to increase as the charging ratio increases. They determined that an optimized heat pipe performance was achieved with an inclination of 30 degrees and a 75% charging ratio. The inclination of the heat pipe plays an essential role in defining its performance due to the role of gravity in driving the condensate back to the evaporator section.

Behera *et al.* (2015) have studied free convective-heat transfer over a fin in a vertical heat sink, using the CFD software package to optimize spacing between the fins. He has plotted contours of temperature and stream function for multiple fin spacing and equivalent Rayleigh numbers. The flow behavior and heat dissipation under corresponding spacing are theoretically calculated for verification. Heat removal is fin effectiveness, and subsequently, overall heat removal effectiveness is defined as fin effectiveness divided by the spacing. Simulations predict increased heat removal and fin effectiveness with increased spacing due to enhanced flow behavior. However, the overall cooling effect is reduced due to the reduced heat transfer area available per unit length of the heat sink. Hence an optimal spacing requires a trade-off between the magnitude of natural convection and the heat transfer area available per unit length of heat sink wall, which increases and decreases with an increase in the fin spacing, respectively.

P. Sakulchangsatjatai *et al.* (2010) presented a model to simulate the thermal performance of an oscillating loop heat pipe and a closed-loop heat pipe. They applied the explicit finite element method. Both the PHPs (pulsating loop heat pipe)were considered to be functioning at top heat mode. The output forecast by the proposed model matched the available experimental data. They determined that increasing the evaporator length resulted in a decrease in heat flux while increasing the inner diameter increased heat flux. It was also concluded that PHP with water as the working fluids had maximum Rth while the one with R123 has the minimum Rth.

Manimaran *et al.*(2018) conducted a series of experiments on copper heat pipes using deionized (DI) water as a working fluid with four different inclination angles. The results showed that the thermal resistance and efficiency of a heat pipe are exaggerated directly by the charging ratio. They displayed that the thermal resistance diminished as the charging ratio increased up to 75% of the evaporator section volume of the heat pipe. Above this span, as the

charging ratio rises, thermal resistance begins to rise. They discovered that better performance was attained with an inclination of 30 degrees and a 75% charging ratio. A vital role is played by inclination in defining heat pipe performance due to the role of gravity in driving the condensate back to the evaporator section.

Hassan *et al.* (2012) examined the consequence of alumina nanoparticles prepared by a two-step method on the performance of heat pipe taking the nanofluid (1 and 3% wt.) of 20-50 nm diameter sizein deionized water and the result which was obtained then compared with heat pipe having deionized water only. Firstly, they took a heat pipe of 10 mm inner diameter, 200 mm brass tube, 50 mm long evaporator, and 50 mm long condenser and displayed that with nanofluid wall temperature declined and the difference between the condenser temperature and evaporator temperature also got reduced. Then, he illustrated that the growth in the thermal diffusivity of the nanofluid was 10%. He discovered that the variation of viscosity of nanofluid was more compared to deionized water and also disclosed that the evaporator temperature was lesser than that of deionized water with increasing heat input.

Senthilkumar *et al.* (2011) studied the behavior of heat pipes operated on aqueous solutions of n-Pentanol at various orientations. The research objective was to do a comparison test between heat pipes working with water and n-Pentanol as working fluids at different inclination angles.The higher performance of the heat pipe was observed when working on n-Pentanol fluid because of the simple reason that the aqueous solutions have a positive gradient of surface tension concerning temperature. Water as a working fluid has some drawbacks, even though it is the most widely used working fluid. So to remove those limitations, the working fluid water can be replaced with a dilute aqueous solution of n-Pentanol. The immense gain of utilizing n-Pentanol is that it has a huge capillary limit and boiling limit, which makes it appropriate for large heat load applications.

Bhullar *et al.* (2017) considered a progressive decline in the performance of heat pipe functioned onsurfactant-free aqueous nanofluids. At higher heat input, much better and more consistent results were obtained compared to lower ones. Also, the use of nanoparticles inflamed the boiling limit and compacted the beneficial contact angle.

Mathew R. *et al.* (2018) recognized the High Energy Advanced Thermal Storage HEATS program which resolved on the advance of a high-temperature latent heat thermal energy storage medium as the major energy storage onboard a bi-modal solar thermal microsatellite. A bi-modal thermal bus proficient in contributing propulsive and electric power to a

spacecraft was before recognized as a capable architecture for microsatellites demanding a substantial delta V. Investigation of prevailing technology illustrated that the use of high-performance thermal energy storage is the enabling technology for such a bi-modal configuration earlier solar thermal studies had recommended the use of high-temperature phase-change materials PCMs such as silicon and boron.

Naghavi *et al.* (2015) issued a detailed evaluation of hybrid applications. It was examined from the experimental literature that heat pipes with latent TES systems for solar applications boosted their efficiency. The numerical research explained the use of 1-D and 2-D simulations. The study involved provides an innovative state-of-the-art, which is mainly related in this case since the publications concerning hybrid systems grew remarkably in the last few years. The current study also describes a different approach to numerical research, by explaining the heat pipe modeling in hybrid systems. Regardless of the system dimensions (1-D or 2-D), the model complexity can be diminished by simulation of the heat pipe as a high thermal conductive solid, for example, reducing the computing costs. The research section's interest in heat pipes and latent TES hybrid technology has enlarged within the last few years. Therefore, the objective of this paper is to deliver modernized guidelines for further research on this technology. The examination classifies the studies according to their application, which makes it easier to spot what previous studies have been carried out, and what further can be done.

D. Yin *et al*. (2014) established a model proficient in anticipating the effect of the filling ratio on the power essential for the start-up of a PHP having one turn. An observation was made that the heat input which is essential to start the oscillatory motion of the working fluid within the PHP enlarged when the FR was increased. The model demonstrated that there is an upper limit of FR above which the PHP cannot start up with the oscillatory movement of working fluid although the heat flux becomes significantly large. Observations were made that for the given PHP, when charging was done with water and ethanol, the upper limits were 76.2% and 78.6% respectively, at an operating temperature of 335K.

Meng *et al.* (2021) examined how to reprocess hot water from a blast furnace slag and converted the thermal energy into electricity using a TEG. From the study some parameters were established, the related parameters that afflicted the TEG performance such as the thermoelectric element length, flow passage length, and water temperature. The power density generated by this system was about 0.93 kW/m2 at 2% conversion efficiency.

Meisel *et al.*(2017) established a design of a multilayer ceramic heat pipe used for high-temperature heat pipe heat exchangers which can be utilized in high corrosive and abrasive environments. To predict the axial heat transfer rate of the thermosyphon a numerical model was established and the results agreed with the experimental data. The working fluid selected was sodium, and the case material was Inconel 600 cladded with ceramic. A thermosyphon heat pipe and a wicked heat pipe were considered for testing. It was examined that the performance of the heat pipe with capillary structure is enhanced as compared to the thermosyphon for the same circumstances.

Research Gaps

Following are the gaps observed while doing the literature survey;

1. The literature survey shows that limited work has been done to investigate the performance of heat pipes.

2. What are the different parameters on which the performance of heat pipe depends all such aspects need a thorough investigation.

3. The literature survey shows that variation in surface temperature of different specimens and their behavior under forced and free convection conditions has not been investigated.

4. The variation of heat transfer coefficient in different conditions with the variation of input parameter has not been investigated.

Research Objectives

Keeping in view the above literature survey the following objects have been formed in the study undertaken.

1. To predict the heat transfer coefficient of heat pipe under natural and forced convection

2. To compare the analytical and experimental heat transfer coefficient for different specimens (Aluminium plugs, Finned aluminum rods, Finned heat pipes) under free and forced convection conditions

3. To study the effect of varying parameters, such as; temperature, input power, and Reynold's number on the performance of different types of heat pipes under free and forced convection

CHAPTER 3: EXPERIMENTAL SETUP AND METHODOLOGY

There are many forms of heat exchangers that are used to transfer heat between two fluids. Heat is transferred between a fluid flowing through a bundle of tubes and another fluid flowing transversely over the pipes outside. In the study undertaken, a cross-flow heat exchanger setup was used to perform the experiments. Various experiments have been performed using different heat pipes and input parameters. A detailed report on the experimental setup and its other components has been provided in the subsequent sections of this chapter. This configuration used is called 'Cross Flow Heat Exchanger' and is shown below.

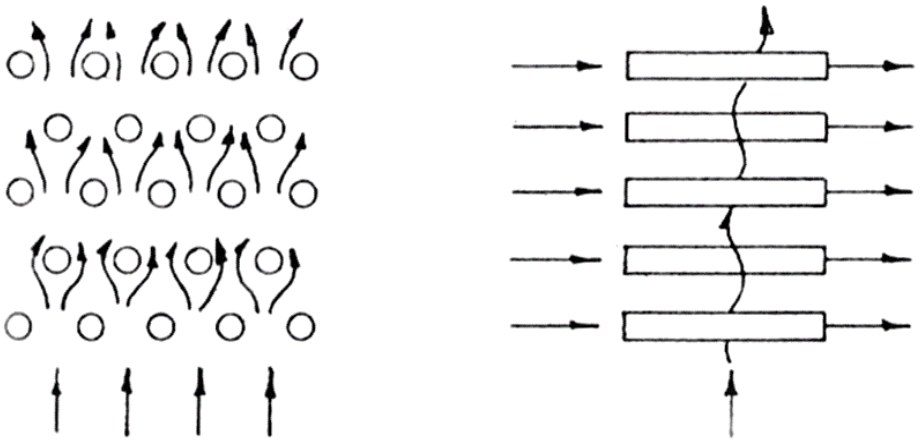

Fig. 3.1: Direction of flow in the cross-flow heat exchanger (P.A Hilton, 2022)

To improve the efficiency of the cross-flow heat exchanger and thereby diminish the physical size for a given heat transfer rate several tube layouts have been created. All the arrangement's purpose is to stimulate turbulence in the fluid flowing across the tube bundle. This is because the overall heat transfer coefficient for a cross-flow heat exchanger is made up of three components. The first component is, the surface heat transfer coefficient for the fluid flowing through the tubes; the second component is, the thermal conductivity and thickness of the tube material; and the third component is the surface heat transfer coefficient for the fluid flowing over the external surface of the tubes. The first two components' enhancement may be accomplished by increasing flow velocity in the pipes and diminishing the tube wall thickness or utilizing a material of higher thermal conductivity.

The third component may be enlarged by raising the stream velocity, thereby raising the external Reynolds Number of each tube. The layout of the tube may be transformed to maximize turbulence, alternatively. This task can be accomplished by confirming that each

row of tubes is located such that turbulence produced by the preceding row is incident upon the next row. A cascade effect is hence produced such that the degree of turbulence rises with the depth of the tube bundle. The consequence of turbulence is to upsurge the surface heat transfer coefficient above the level accomplished byincreased Reynolds Number alone. In case the fluid flowing over the surface of the tubes is a gas, then the effective heat transfer coefficient maybe additionally increased by the use of extended surfaces, for example, fins. We know that cross-flow heat exchangers exist in various forms throughout the industry, and engineers and technologists must have information about the performance of such units. The experimental setup involves an air duct, vertically mounted 65*150 mm cross-section with bell mouth intake at its upper end, and is equipped with a front cover of opaque plastic with a central opening of 200 mm in length to accept heat exchanger and tube carrier plates. Centrifugal blower of 1.1kW power input three-phase is mounted on the epoxy-coated welded steel frame while the air duct is directly mounted on the frame and a fan speed control inverter to control the speed of air is mounted on the fan frame. Setup is equipped with a facility to adjust the three-phase output from zero to 50 Hz. The actual setup used in the experimentation has been shown in Fig. 8.

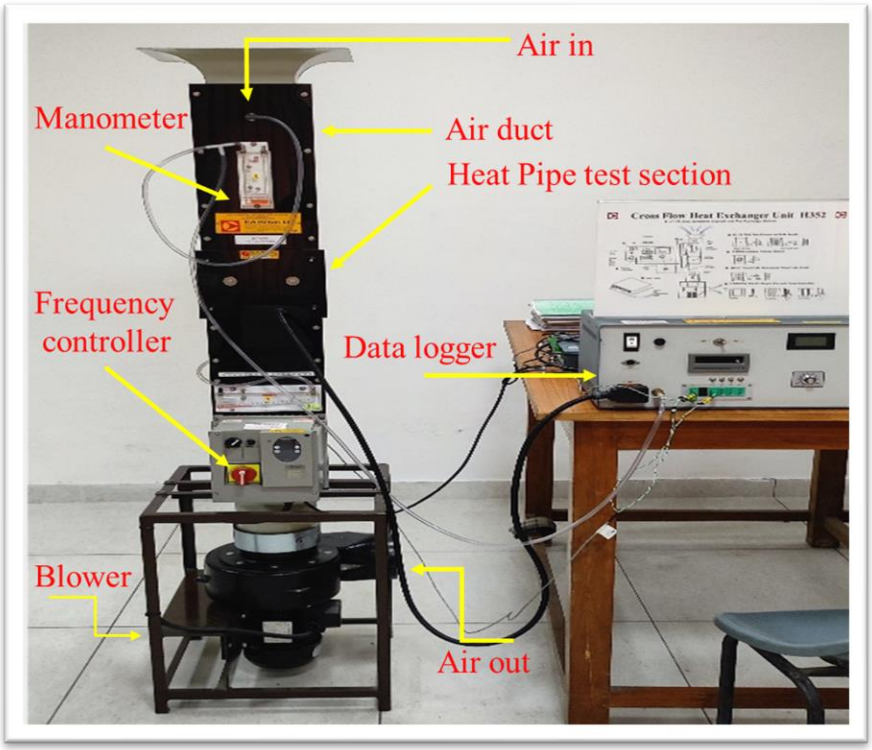

Fig. 3.2: Cross flow heat exchanger with heat transfer unit setup

3.1 Instrumentation and control

In the experimental device used, all the electronic instrumentation and control are housed inside a plastic-coated steel console. There is a digital electronic thermometer with 0.1°C resolution on the console which indicates element surface temperature via a biased switch and, the duct air temperature. The voltage across the active element heater is indicated by an analog voltmeter which has a range from 0 to 70V. The rotary variable transformer regulates the voltage across the active element heater between 0 and 70V. A duct-mounted inclined manometer records intake depression i.e. it is used for measuring the pressure of air at the inlet and has a range from 0 to 100 mm H_2O. A duct-mounted inclined manometer that has a range of 0 to 20 mm H_2O is installed below the heat exchanger. A voltage switch controls the maximum voltage from the rotary voltage transformer and has a 70V maximum supply for the 8- pin heater and thermocouple plug and a 35V for the 7-pin accessories socket.

3.2 Plain tube heater &tube bundle

In this arrangement, a clear plastic plate with a centrally drilled hole to accept the single active element which has plate dimensions such that it snugly fits the 200 mm opening in the air duct is called a single tube plate. Similarly, a clear plastic plate with 27 fixed plastic tubes of 16 mm nominal diameter arranged on an equilateral triangular pitch of 32 mm between centers in which tubes form six rows, and near the center of each row is a dummy tube that may be removed and replaced with the active element is called a multi-tube plate.

3.3 Local heat transfer element

A local element is defined as a non-metallic test cylinder coated with an electrically conducting glass cloth and incorporating a surface thermocouple. A plastic plate with an access hole and retaining clips that fit the duct-aperture enabling the local element to be placed in the duct air stream is called a carrier plate. A graduated degree plate enables positioning of the thermocouple relative to airflow direction.

3.4 Finned tube heater & tube bundle

In this arrangement, a clear plastic plate with 14 copper finned tubes of 25.4 mm fin diameter and 12.7 mm root diameter and these are arranged on an equilateral triangular pitch of 30 mmbetween centers in which tubes form four rows, and near the center of each row is an identical dummy tube that may be removed and replaced with the active element is termed as a finned tube plate. In this type of arrangement, an active element that is electrically heated

(maximum 70V) thick copper cylinder of nominally 12.7 mm diameter and 55 mm length is used.The external surface has a copper finning of 25.4 mm diameter identical to dummy tubes. Extreme ends are insulated to reduce errors due to wall effects. The integral thermocouple senses surface temperature.

3.5 Free and Forced convection heater plates

In a flat plate heat exchanger**,** the carrier plate fits into the duct aperture and incorporates a 100 W heater mat and flat aluminum plate with a surface thermocouple.A single plug connects to the 70 V power source and temperature measurement console. Similarly, in a pinned plate heat exchanger a carrier plate fits into the duct aperture and incorporates a 100 W heater mat and flat aluminum plate with 25 pins of 12.7 mm diameter, thermocouples are attached to the heater surface at three points on the extended surface of the pins. Whereas in a finned plate heat exchanger, the carrier plate fits into the duct aperture and incorporates a 100W heater mat and finned aluminum plate, thermocouples are attached to the heater surface and at three points on the extended surface of the fins.

3.6 Specimen

There are three different specimens used during the experimental work, namely:

1. Aluminum plugs
2. Finned aluminum rods
3. Finned heat pipes

1. Aluminium plugs

This specimen used has a diameter of 9.5 mm and 55 mm in length. Aluminum heat pipes allow easy transportation of a large amount of heat with a small amount of energy loss. The specimen image has been shown in Fig.9

Fig. 3.3: Aluminum plugs

2. Finned aluminum rods

This specimen has a diameter of 9.5 mm and 150 mm in length. The fins attached to its upper portion are used to enhance the heat transfer area. The specimen has been shown below in Fig.10

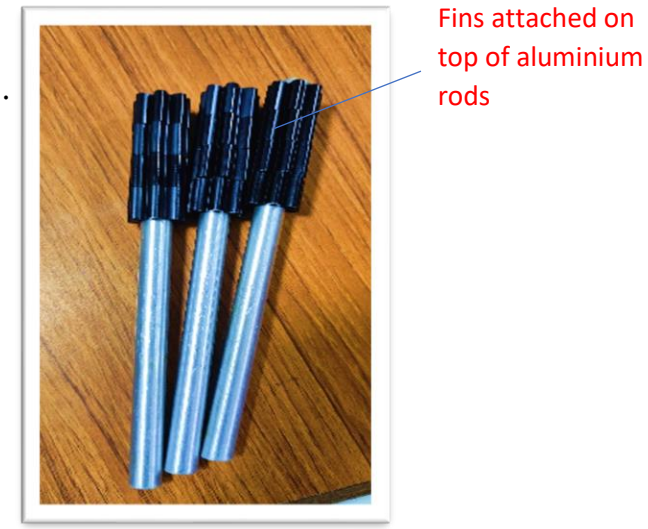

Fig. 3.4: Finned aluminum rods

3. Finned heat pipes

This specimen used has a diameter of 9.5 mm and 150 mm in length. It is made up of copper and its high thermal conductivity allows heat to pass through quickly. The specimen image has been shown below in Fig.11

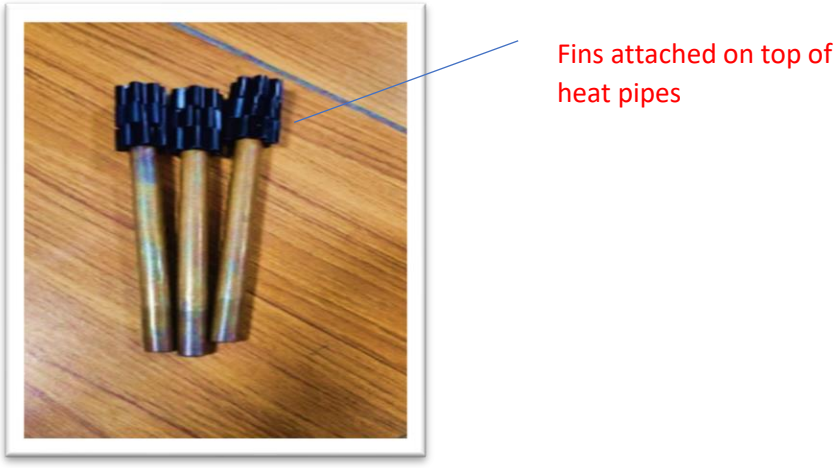

Fig. 3.5: Finned heat pipes

3.7 Description of the experimental setup

A detailed description of the different components of the experimental setup has been provided in Table 3.

Table 3. The components of the experimental setup with their features(P.A Hilton, 2022)

Device components	Features
Air duct	1) Vertically mounted duct of 65*150mm and 1.2m long. 2) Fan runs at variable speed air flow rate as shown in Fig.13, controlled by inverter. 3) It has an opaque plastic front cover and is situated at approximately mid-position. 4) Along its length is a 200 mm long opening, it is bell-shaped as shown in Fig.12
Heater control	1) A variable rotary transformer controls the voltage supplied across the active element heater as shown in Fig 15. 2) A maximum power of 70V is supplied to the element from a fused, earthed, and thermally protected supply. 3) Output is fused and mounted on the instrument console.
Voltage switch	1) A voltage switch controls both maximum voltage from heater control and output socket to which power is applied. 2) In the 70V position power is supplied to the 8-pin socket and in the 35V position, power is supplied to 7 pin socket as shown in Fig.15
Electronic temperature Indicator	1) This gives the temperature of the surface (T1) of the active element and air temperature (T2) within the duct as shown in Fig.15. 2) Resolution of the instrument is 0.1 degrees Celsius.
Voltmeter	1) This is situated on the console and indicates voltage supplied across active elements as shown in Fig 15. 2) Range is 0 to 70 V
Manometer	1) There are two manometers provided on the duct to measure intake depression, one shown in Fig.14

Fig. 3.6: Air duct

Fig. 3.7: Centrifugal blower

Fig. 3.8: Air flow control

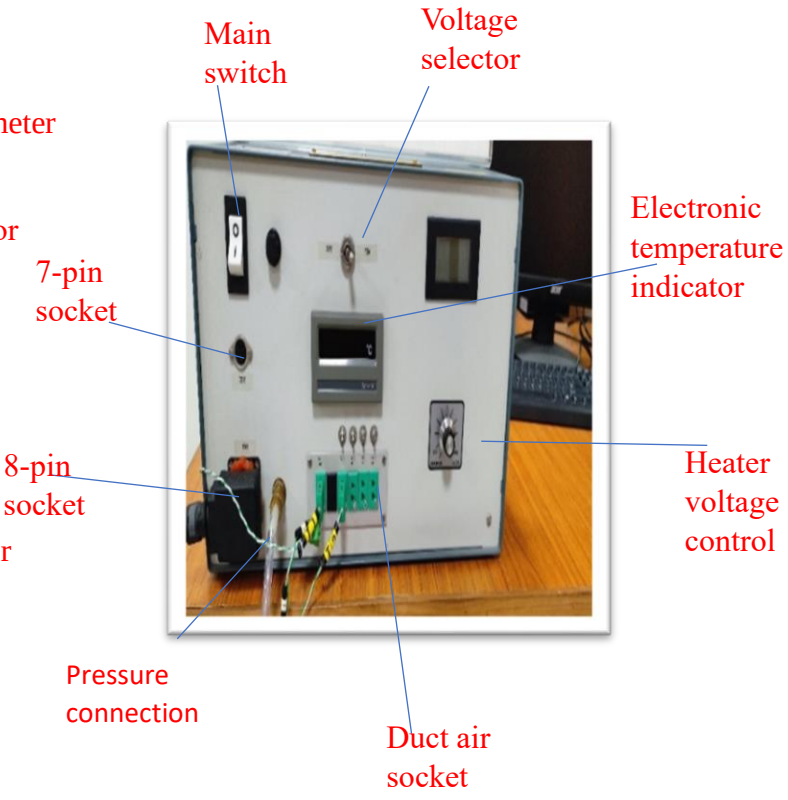

Fig. 3.9: Console

4.1 Safety devices

The safety devices which are involved, consist of a wire mesh finger guard, fan speed control inverter, internal relay, miniature circuit breaker, residual current circuit breaker, and active element heater fuse. A wire mesh debris guard is positioned at the entrance to the fan. The access to rotating parts is prevented by a wire mesh finger guard at the fan exit. The fan speed control inverter has in-built current limiting protection of both itself and the fan and error messages are displayed on the LCD. Active element high-temperature protection is done through the actively heated element surface thermocouple (T1) connected to the electronic temperature indicator and pre-set relay via the 8-pin and 7-pin plugs on the console. The biased switches in the at-rest position maintain a connection to the surface temperature (T1) thermocouple. If the active element's surface temperature exceeds approximately 100°C, the internal relay opens and cuts off the power supplied to the element. When the temperature is reduced below 100°C, power is automatically restored to the element. The main switch is also a thermal circuit breaker. If an electrical overload should occur whilst in use, the breaker will operate and isolate the unit from the switch onwards (the digital thermometer display will be extinguished). The unit should be disconnected from the mains supply and the cause of the overload determined. The 30 mA R.C.C.B. is mounted on the rear of the console. Under normal operation, it should be kept inthe 'ON' position and not used as an 'ON/OFF switch. The R.C.C.B. will trip to the 'OFF' position if an earth fault occurs, isolating the console and fan from thesupply if the R.C.C.B. trip, the main supply to the unit should be disconnected, and the cause of the fault to be determined. The R.C.C.B. can then be reset to the 'ON' position and the unit can be operated. Every three months the R.C.C.B. should be checked by a competent person. To do this, switch on the main switch and run the fan. Push the 'TEST' button on the R.C.C.B. and check the fan and console areisolated. If the power remains on, the R.C.C.B. is faulty and will need to be replaced by a qualified electrician. The active element heater fuse is situated on the console and is a 2A replaceable glass cartridge unit. The heater elements operate at a maximum of 70V for safety reasons and the maximum current normally taken will be approximately 1.5A. Fuse failure will normally indicate a fault in the low voltage circuit after the internal mains transformer.The cause should be investigated. Replacement of an active element fuse is achieved by first isolating the unit from the mains. The fuse holder is unscrewed and a replacement fuse is inserted in the cap. The cap and fuse are refitted and screwed home.

4.1 Operation and methodology

During the operation phase of the experimental device, we have two control parameters these are heater control and air velocity control. In heater control, the instrument console has two controls, the variable transformer, and the voltage switch. In the 70V position, power is supplied only to the large 8-pin socket on the extreme left of the console. In the 35V position, power is only supplied to the 7-pin socket. In both cases, the variable transformer will control the voltage supplied between Zero Volts and the maximum, either 70 or 35 Volts. Rotation of the dial clockwise will increase the voltage and power input, and anti-clockwise will reduce the voltage and power input whereas, in air velocity control, the duct air velocity is controlled directly by the fan speed. This in turn is controlled by an inverter thatvaries the frequency of the three-phase supply to the fan motor.

4.1 Obtaining Stable Conditions

Stable conditions are indicated by a constant active element surface temperature. With the active element in any of the tube plates and the tube plate mounted in the air duct, thefan should be started. Adjust the fan speed so that the required intake depression is indicated on the duct manometer. With the active element plugged into the console, depress the console main switch and slowly increase the active element heater voltage. The indicated temperature will be seen to rise. Adjust the heater voltage in increments until the desired surface temperature is achieved. If the surface temperature exceeds approximately 100°C the voltage needle will swing to zero as the power is cut off by the thermal protection relay. When the element cools to below 100°C power will be restored. If the duct air velocity is not increased, or the heater power input is reduced, the thermal protector will continue to cycle in this manner. And the temperature indicator will be extinguished. Restore the power by resetting the RCCB switch.
Rotate the console Voltage Control to increase the indicated voltage and observe the Surface Temperature(T1) should increase. With zero airflows, the heater temperature may rise to the 100°C cut-out point and the voltage should fall to zero at this point. Now, depress the duct air temperature (T2) biased switch and the Temperature Indicator will display temperature T2. Temporarily remove the probe and subject it to hand heat. With the T2-biased switch depressed, the T2 temperature should be increasing.

CHAPTER 4: THEORETICAL ANALYSIS

In this section, we will try to study and implement all the equations which are used to determine the performance of heat pipes.

4.1 Determination of the Duct Air Stream Velocity

By application of Bernoulli's equation between the pressure tapping point and the external atmosphere, the following equation may be obtained-

$$U = \sqrt{\frac{C_d 2 \,\mathrm{Im}\, gHRT_a}{Pa}} \tag{1}$$

Where *R* is the specific gas constant for air.

For the intake type used on the duct, *Cd* is taken as 0.98. Substituting in the equation for the known quantities gives:

$$U = {}^{74{\cdot}294}\sqrt{\frac{HT_a}{P_a}} \ \text{m s}^{-1} \tag{2}$$

Note that the velocity obtained is the velocity existing in the unobstructed duct. Where the obstruction is small as in the case of the single tube, the effects of such a blockage may be ignored. However, when the multi-tube plate is in position, the blockage effect must be accounted for andin fact, the velocity through the minimum area available to flow is taken. For the plain multi-tube plate this results in an effective velocity through the tube bundle of,

$$U' = 2.393\, U \tag{3}$$

This equation is used under natural convection conditions

$$Gr = \frac{g\beta(T_C - T_e)L^3}{\nu^2} \quad (4)$$

This equation is used under natural convection conditions for calculating the Prandtl number

$$Pr = \frac{\mu Cp}{k} \quad (5)$$

This equation is used for calculating the Rayleigh number under free convection

$$Ra = Gr * Pr \quad (6)$$

This equation is for a vertical cylinder under natural convection(external flow)

$$Nu = 0.59(Ra)^{0.25} \quad (7)$$

This equation is used for calculating the Nusselt number

$$Nu = \frac{hL_c}{k} \quad (8)$$

This equation is used for calculating the Reynold number under forced convection

$$\mathrm{Re} = \frac{\rho VD}{\mu} \quad (9)$$

This equation is used for calculating average bulk air temperature

$$T_b = \frac{T_{b_1} + T_{b_2}}{2} \quad (10)$$

$T_{b1=}$ inlet temperature of the air, T_{b2}= outlet temperature of the air

This equation is used for calculating the experimental heat transfer coefficient under forced convection

$$h_{\exp} = \frac{Q_{in}}{A(T_\omega - T_b)} \quad (11)$$

This equation is used for calculating the film temperature avg. of wall and air temperature

$$T_f = \frac{T_\omega + T_a}{2} \quad (12)$$

This equation is used for calculating the experimental heat transfer coefficient under free convection

$$h_{\exp} = \frac{Q_{in}}{A(T_C - T_e)} \quad (13)$$

This equation is used for calculating the Nusselt number under forced convection

$$Nu = 0.664(\mathrm{Re})^{0.5}(Pr)^{0.33} \quad (14)$$

Churchill and Chu's relation is used for calculating heat transfer coefficient under free convection :

$$Nu^{1/2} = 0.825 + \frac{0.387\ Ra^{1/6}}{[\,1+(0.492/Pr)^{9/16}\,]^{8/27}} \quad \text{for } 10^{-1} < Ra < 10^{12} \quad (15)$$

Churchill and Bernstein's relation is used for calculating heat transfer coefficient under forced convection :

$$Nu = 0.3 + \frac{0.62\ Re^{1/2}\ Pr^{1/3}[\,1+(Re/282000)^{5/8}\,]^{4/5}}{[\,1+(0.4/Pr)^{2/3}\,]^{1/4}} \quad \text{for } 10^{2} < Re < 10^{7} \quad (16)$$

This equation is used for calculating the overall heat transfer coefficient based on various thermal resistances at external surfaces of the evaporator section and condenser section and inside a container of the heat pipe and all equations from 19 to 23 are used in the calculation

$$1/U = R_h + R_{HP} + R_c = 1/h_h + 1/U_{HP,p} + 1/h_c \quad (17)$$

$$h_h = 4.55\ Re^{0.733}\ Pr^{0.362} \quad (18)$$

$$Re = \rho v D_h / \mu \quad (19)$$

$$v = 4v_f / \pi (D^2 - d_o^2) \quad (20)$$

$$D_h = (D^2 - d_o^2)/(D + d_o) \quad (21)$$

These equations 24, and 25 are used for calculating the effective length of the heat pipe in equation 26

$$R = T_e - T_c / Q \quad (22)$$

$$k_{eff} = L_{eff} / A*R \quad (23)$$

$$L_{eff} = 0.5L_e + L_a + 0.5L_c \quad (24)$$

Table 4: Properties of working fluids for low-temperature applications. (Wallins,2012)

MEDIUM	**Melting Point (°C)**	**Boiling Point at Atmospheric temperature (°C)**	**Useful Range(°C)**	
Helium	-271	-261	-271	-269
Nitrogen	-210	-195.8	-203	-160
Ammonia	-78	-33	-60	100
Pentane	-130	28	-20	120
Acetone	-95	57	0	120
Methanol	-98	64	10	130
Ethanol	-112	78	0	130
Water	0	100	30	200
Mercury	-39	361	250	650
Sodium	98	892	600	1200
Lithium	179	1340	1000	1800
Silver	960	2212	1800	2300

4.2 Vapour pressure of viscous limit

The minimum pressure at the condenser section of the pipe might be shallow at the low-temperature range of operation of the working fluid, mainly when starting the heat pipe. The vapor pressure drop between the end of the evaporator and the condenser represents a restriction in operation. At low operating temperature, the saturation vapor pressure may be of the same order of magnitude as that of the pressure drop required for helping the vapor flow in the heat pipe. It is expected that the vapor pressure will be minimal and reaches zero at the condenser. in this condition which is an inadequate pressure available to drive the vapor, the limitation of the heat pipe to transport heat is termed a viscous limit.

$$Q_{viscous\ limit} = \pi P r_v^4 h_{fg}\, \rho_v / 16 \mu_v L_{eff} \quad (25)$$

4.3 Sonic limit

Sonic Limit is defined as the condition when the velocity of the vapor present in the heat pipe reaches sonic values, and the condenser temperature cannot further increase the heat transfer rate. This condition is primarily concerned with liquid metal and is defined as a choked condition, and the limit is called the sonic limit.

$$Q_{sonic} = \rho_v h_{fg} A_v c_o / (2(\Upsilon+1))^{0.5} \quad (26)$$

4.4 Entrainment limit

Entrainment Limit is when the vapor velocity rises with temperature and can become very large to generate a shear force that affects the liquid return flow from the end of the condenser region to the last point of the evaporator section causing entrainment of the liquid by the vapor. This limitation of the heat transport capability is defined as the entrainment limit.

$$Q_{entrainment\ limit} = A_v h_{fg} \left(\sigma \rho_v / 2R_{h,w}\right)^{0.5} \quad (28)$$

4.5 Boiling limit

The temperature decreased along the wick structure in the evaporator zone and escalates with the evaporator heat fluxes. A critical point arrives when the temperature difference exceeds the degree of superheat sustainability about nucleate boiling conditions. Boiling inside the wick structure interferes with the circulation of liquid. This mainly leads to dry out, which can trigger evaporator containment burning in the event of continuous heat flux heating.

$$Q_{boiling\ limit} = 2\pi L_e k_{eff}\, \Delta T_{crit} / \ln (r_i/r_v) \quad (29)$$

4.6 Capillary limit

The capillary limitation is the maximum pumping pressure the heat pipe can hold and still return the condensate through capillary forces. The driving force for fluid movement within the heat pipe is given by the capillary force produced within the wick of the heat pipe.

$$Q_{\text{capillary limit}} = \frac{\frac{2\sigma}{r_c} - \rho_1 g L_{eff} \sin \Phi}{\frac{\mu_1 L_{eff}}{\rho K A_1 h_{fg}} + \frac{8\mu_v L_{eff}}{\rho_v \pi r_v^4 hfg}} \quad (30)$$

4.7 Fins

Fins or extended surfaces represent the critical phenomenon of conduction or convection, i.e.,heat is transferred by conduction from the solid and convective heat transfer from the solid boundary. Fins increase the rate of heat transfer between substantial and flowing fluid. There are different types of fins like annular fins, pin fins, straight fins, etc. The selection of particularfin specifications depend upon factors like weight space available, the fabrication cost of fabrication material, and overall cost. So, by taking all these factors into consideration design ofthe fin is finalized.

4.8 Types of heat pipes

There are great amounts of variations done in heat pipe technology due to their versatile applications. Depending on their applications, there are many kinds of heat pipes basedfor different purposes, and a few are shown here namely:

4.8.1 Gravity-assisted heat pipes

(a) thermosyphon

(b) two-phase flow thermosyphon

4.8.2 Capillary heat pipes

(a) cylindrical heat pipe

(b) loop heat pipe

(c) flat-plate

(d) capillary pumped loop

4.8.3 Other heat pipes

(a) rotating heat pipes

(b) pulsating heat pipes

Table 4.1: Types of heat pipes based on their application(Adil Abbas Alwan,2020)

There are different types of heat pipes based on their applications:

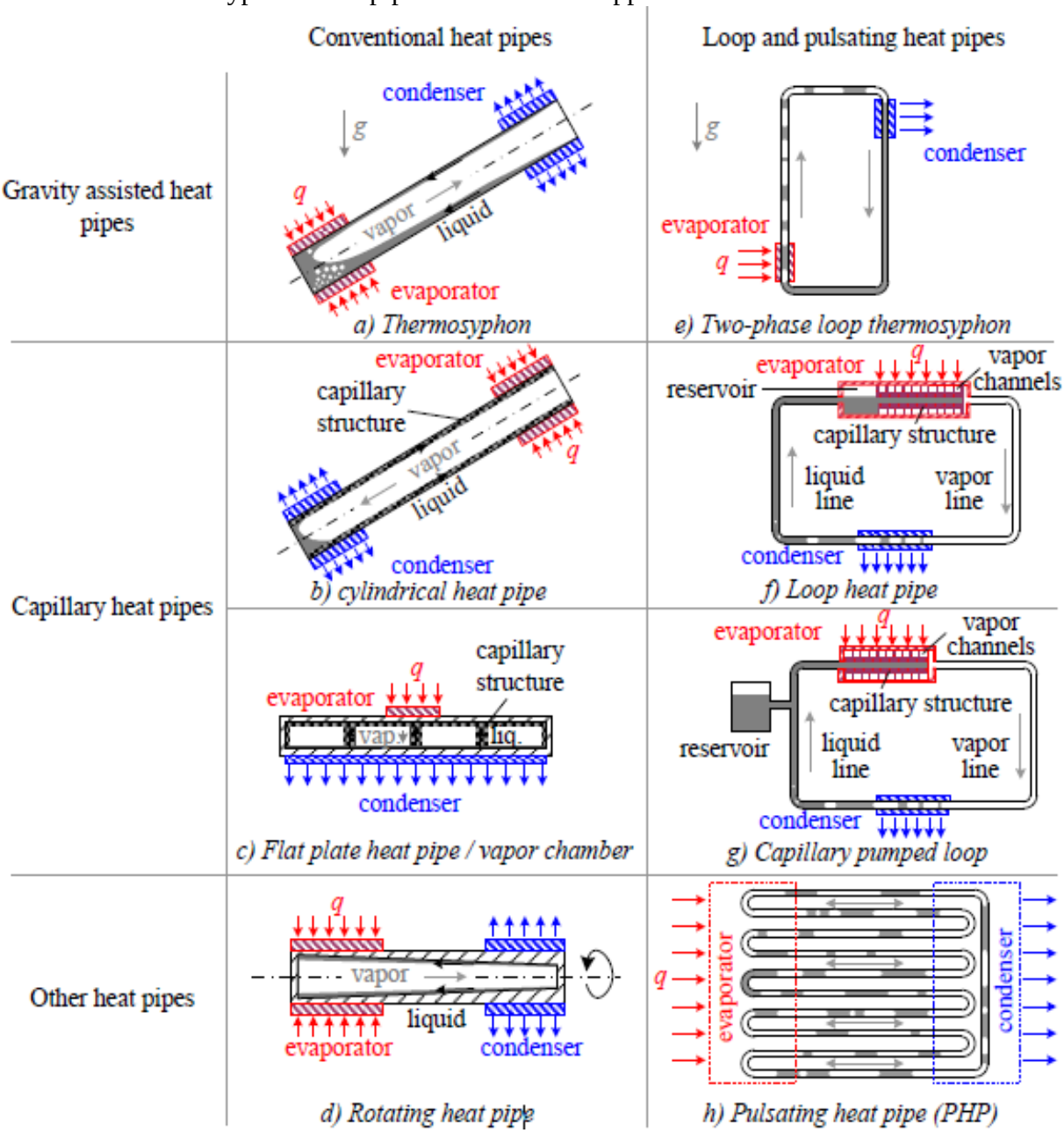

Table 4.2: Various categories of heat pipes and their operating range. (A. Faghri,2020)

Some other types of heat pipes with their operating range, applications, limitations, and features.

Type	Features	Limitations	Applications	Operating temp. (K)
Tubular heat pipes	Simple and effective passive operation.	Requires fresh air stream for optimum operation.	Injection molds and air-to-air heat pipe heat exchangers.	218–453
Variable conductance heat pipes (active control)	Superior heat source and temperature control are possible.	The requirement for supplementary power is there.	Accurate satellite temperature adjustment and elimination of heat from radioactive waste.	268–338
Thermal diodes	Heat flow is Unidirectional.	Difficulty in retrofitting the system.	Gamma-ray gathering of solar gain for space heating.	273–398
Pulsating heat pipes	Growth and collapse of the driving force are there	Increased cost and weight due to inflexible metallic pipe material.	Electronic and central processing unit cooling systems.	273–378
Micro heat pipes	Iso- thermalization and flaccid operation.	Lower heat transfer ability compared to its counterparts	Cooling laser diodes and thermal control of ceramic chip carriers.	313–343

CHAPTER 5: RESULTS AND DISCUSSION

5.1 Variation of surface temperature and temperature difference under natural and forced conditions:

In Fig. 5.1, we can observe that as we are increasing the heat input the surface temperature of the specimen is increasing in all three cases which is a natural phenomenon because as we increase the heat given the surface temperature will rise.

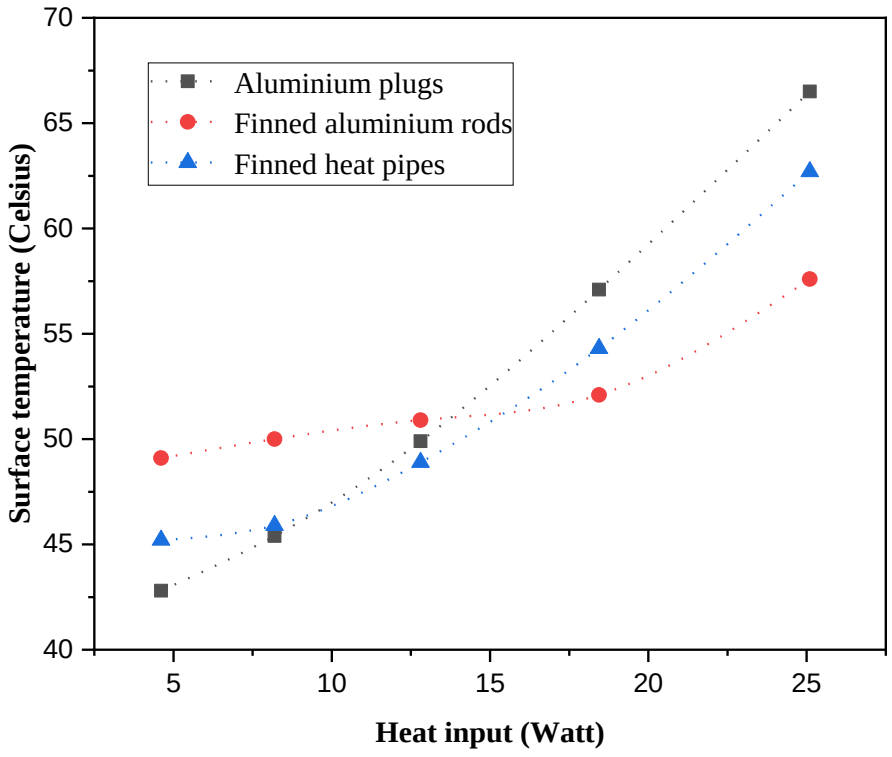

Fig. 5.1: Variation of surface temperature with heat input(natural convection)

Similarly in the case of forced convection as the input power is increasing the surface temperature of the specimen will increase as shown in Fig. 5.2. However, the increase in the case of finned heat pipes was more as compared to the other two because the thermal conductivity of copper is more than aluminum.

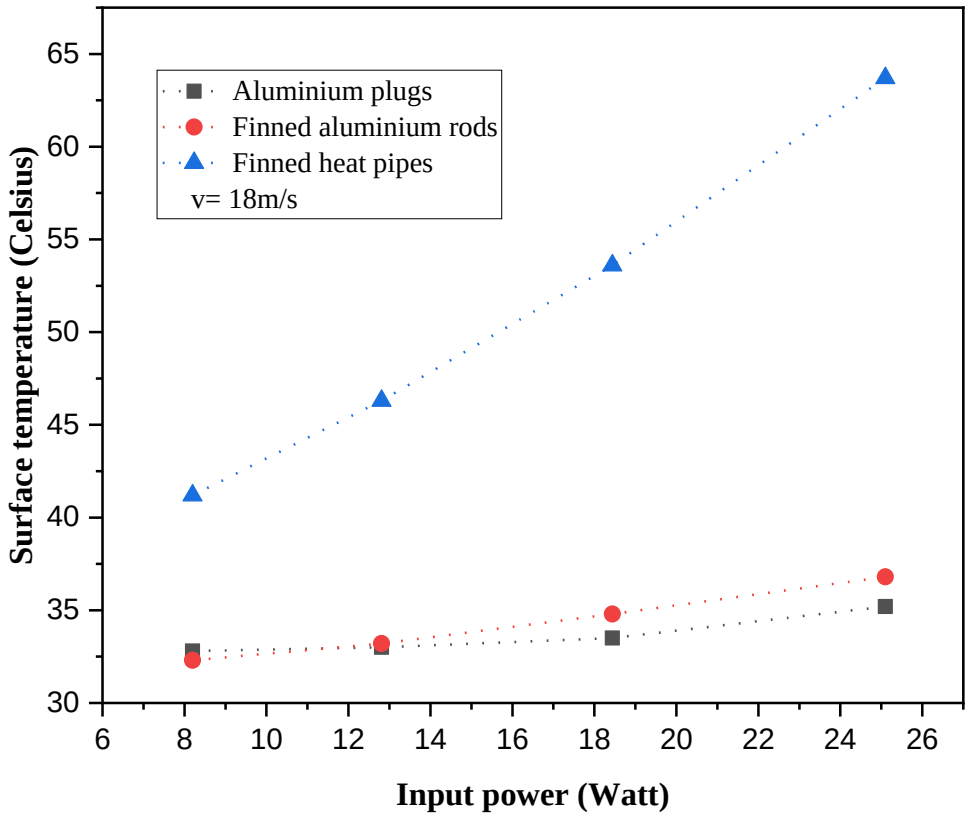

Fig. 5.2: Variation of surface temperature with heat input(forced convection)

In this case, as the input power is increasing the temperature difference is also increasing because as the temperature of the surface is increasing with input power and ambient temperature being approximately constant so the difference will increase as shown in Fig. 5.3.

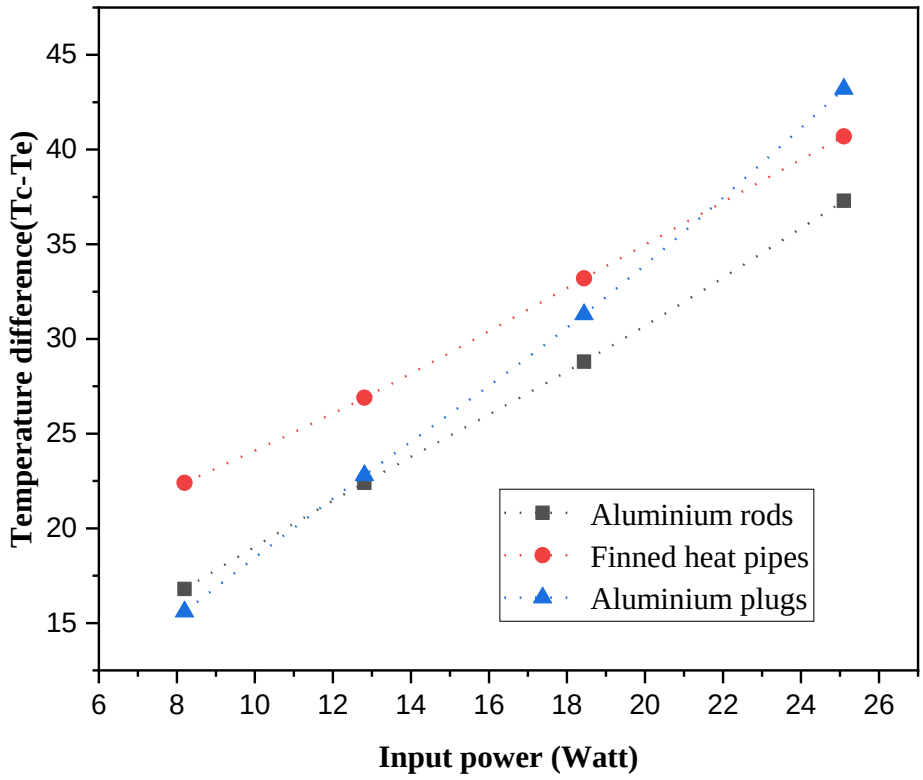

Fig. 5.3: Variation of temperature difference with input power(natural convection)

In this case of forced convection, the velocity of air was kept constant at approximately 9m/s and it was observed that the temperature difference was increasing with input power because the surface temperature is increasing and ambient temperature is approximately constant as shown in Fig. 5.4.

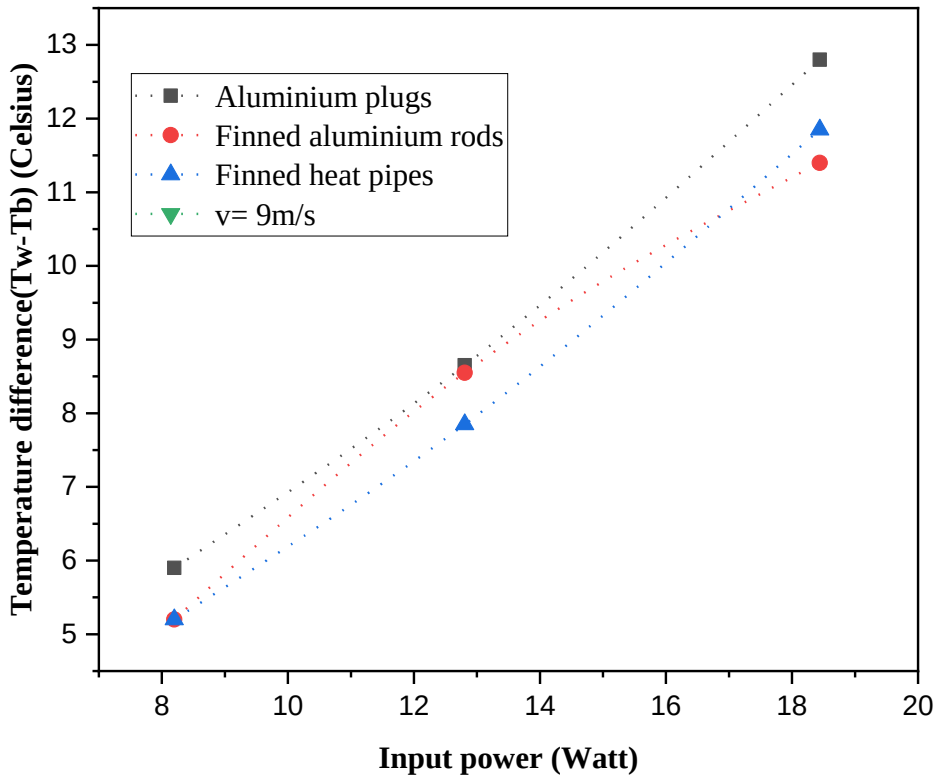

Fig. 5.4:Variation of temperature difference with input power(forced convection)

5.2 Variation of non-dimensionless numbers under natural and forced convection conditions

In this case, as we increase the film temperature the Rayleigh number increased as we know that the Rayleigh number is directly proportional to the temperature difference and the temperature difference was increasing so it will increase with surface temperature as shown in Fig. 5.5.

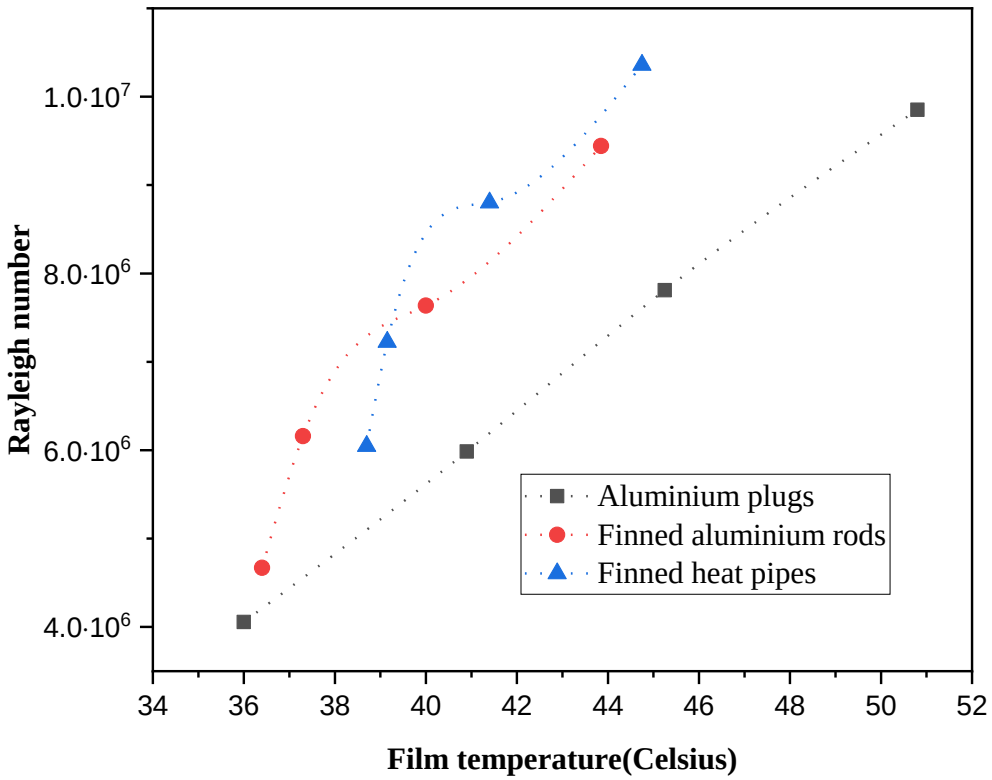

Fig. 5.5: Variation of Rayleigh number with film temperature

In this case of natural convection, it was observed that the Nusselt number was increasing with the Rayleigh number in an almost linear manner because we know that for natural convection the Nusselt number is a function of Grashoff and Prandtl number, and for all the three specimens the difference in film temperature was very less due to which the properties had very less difference hence it increased in an almost linear manner for all the three specimen as shown in Fig. 5.6.

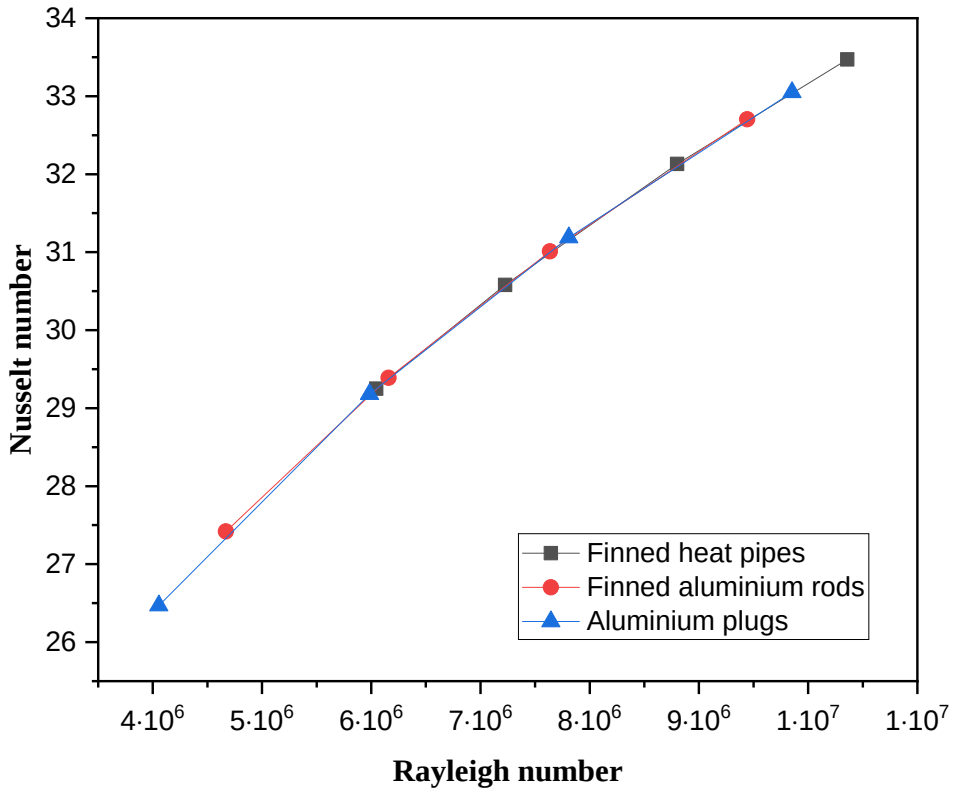

Fig. 5.6: Variation of Nusselt number with Rayleigh number

In the case of forced convection, the Nusselt number is a function of Reynold and Prandtl number due to which the Nusselt number was observed increasing linearly with Reynold number for all the three specimens and also because the film temperature has very less difference as shown in Fig. 5.7.

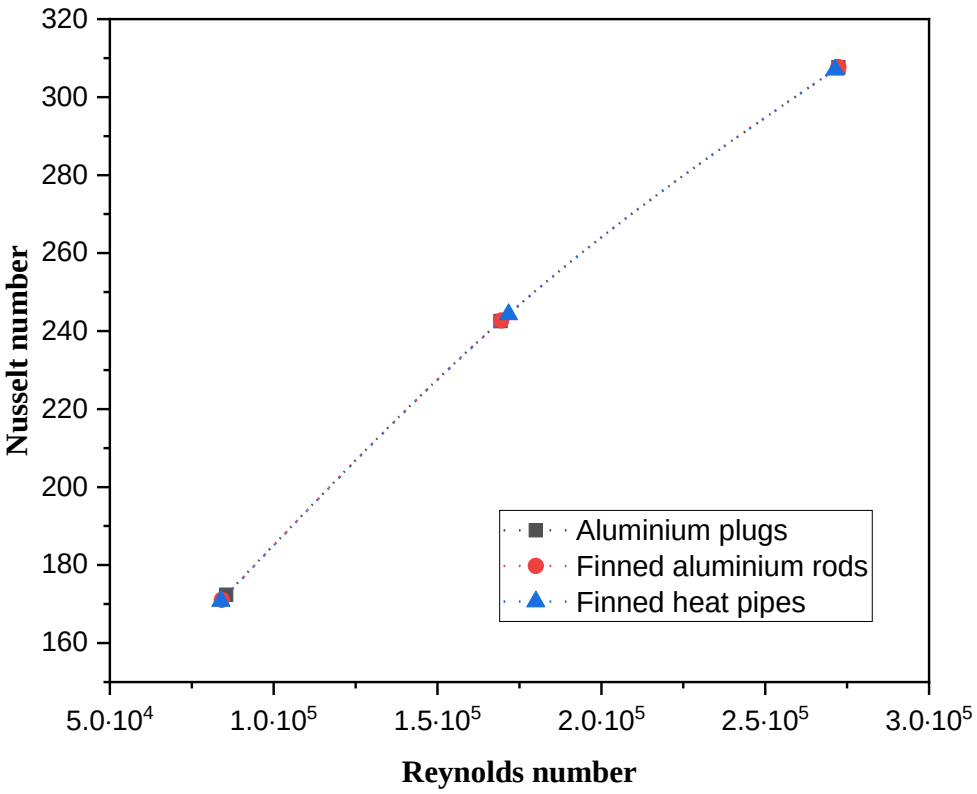

Fig. 5.7: Variation of Nusselt number with Reynold number

In the case of natural convection, as we increase the film temperature the Nusselt number started to increase in an almost linear manner for aluminum plugs and in a curvilinear manner for the finned aluminum rods and finned heat pipes as shown in Fig. 5.8.

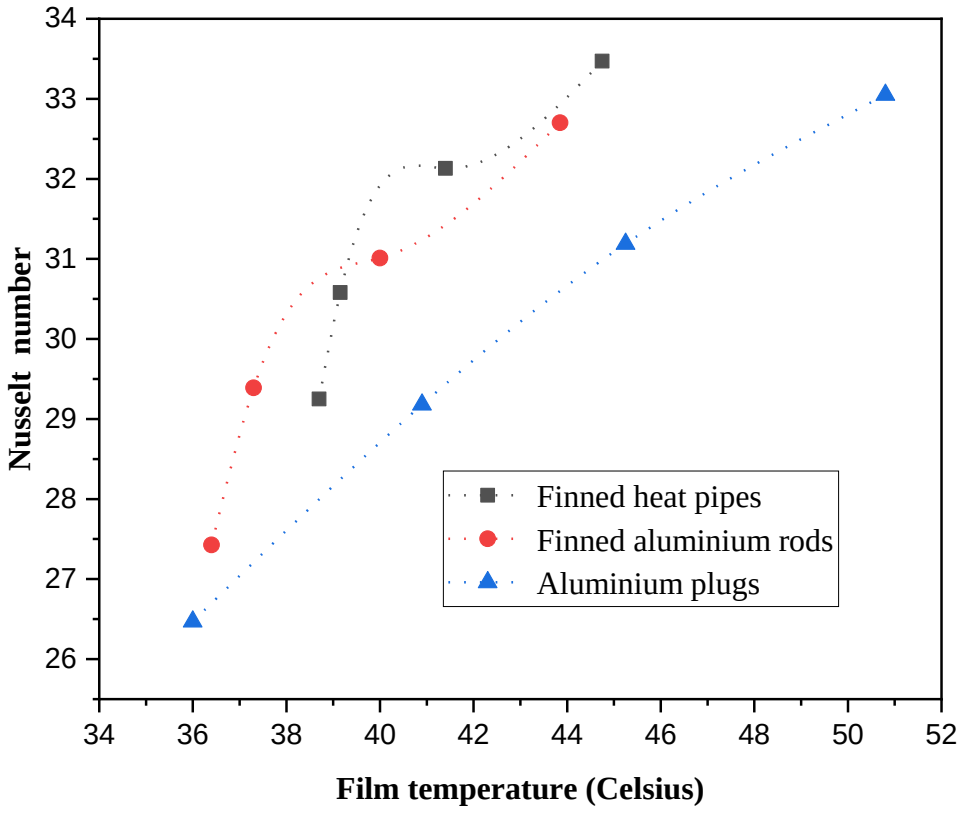

Fig. 5.8: Variation of Nusselt number with film temperature

5.3 Variation of heat transfer coefficient with temperature difference :

In this case of forced convection as we increase the heat input with velocity kept constant at 18m/s it was observed that the heat transfer coefficient increased with an increase in ΔT however in the case of aluminum plugs it first increased and then decreased as shown in Fig. 5.9.

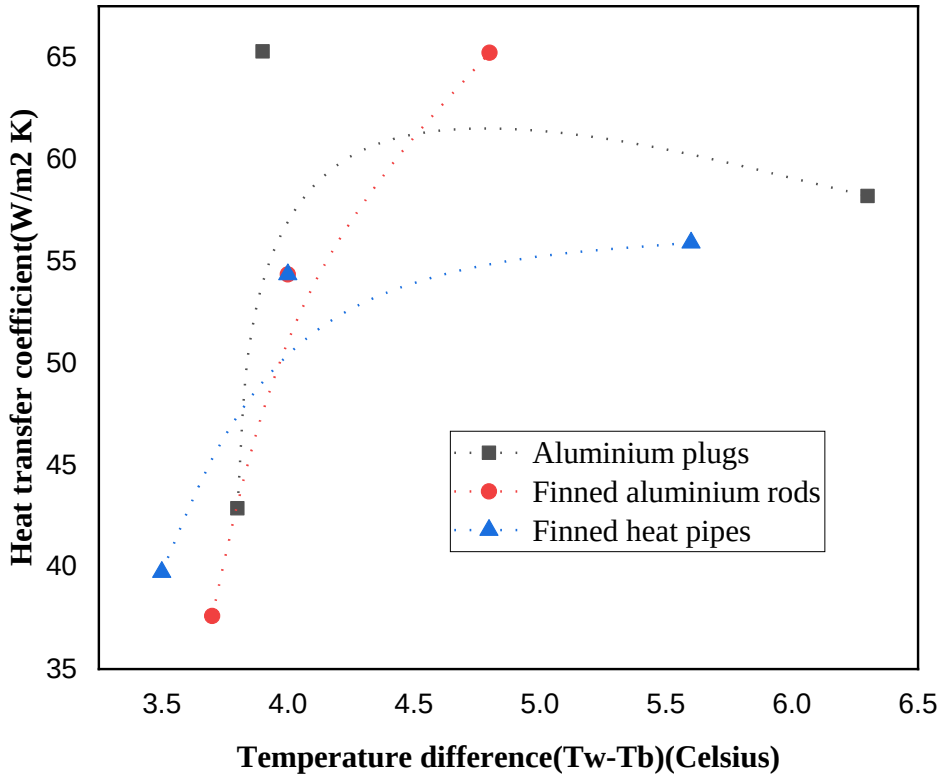

Fig. 5.9: **Variation of temperature difference vs heat transfer coefficient (forced convection)**

In this case of natural convection, it was observed that as we increase the heat input, the heat transfer coefficient increased with the increase in ΔT in an almost linear manner, and the maximum increase of heat transfer coefficient with ΔT was observed in the case of finned heat pipes as shown in Fig. 5.10.

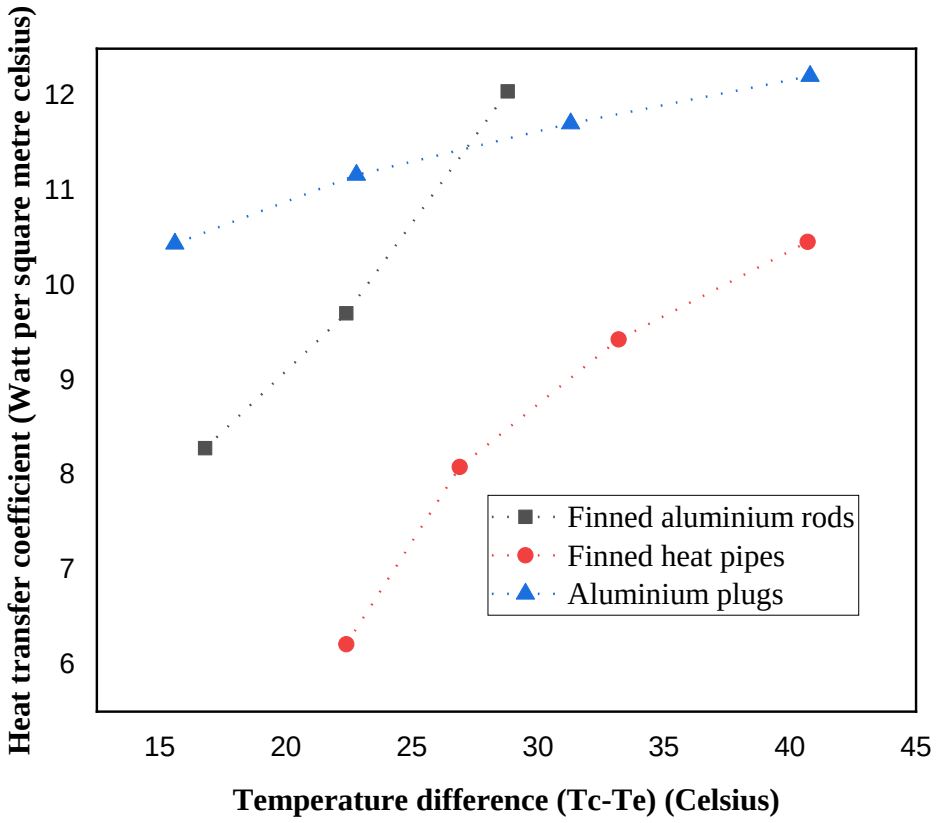

Fig.5.10: Variation of temperature difference vs heat transfer coefficient(natural convection)

5.4 Variation of heat transfer coefficient analytical vs experimental under natural and forced convection conditions:

In the case of aluminum plugs under natural convection, the variation between heat transfer coefficient analytical and heat transfer coefficient experimental is shown in Fig.5.11.

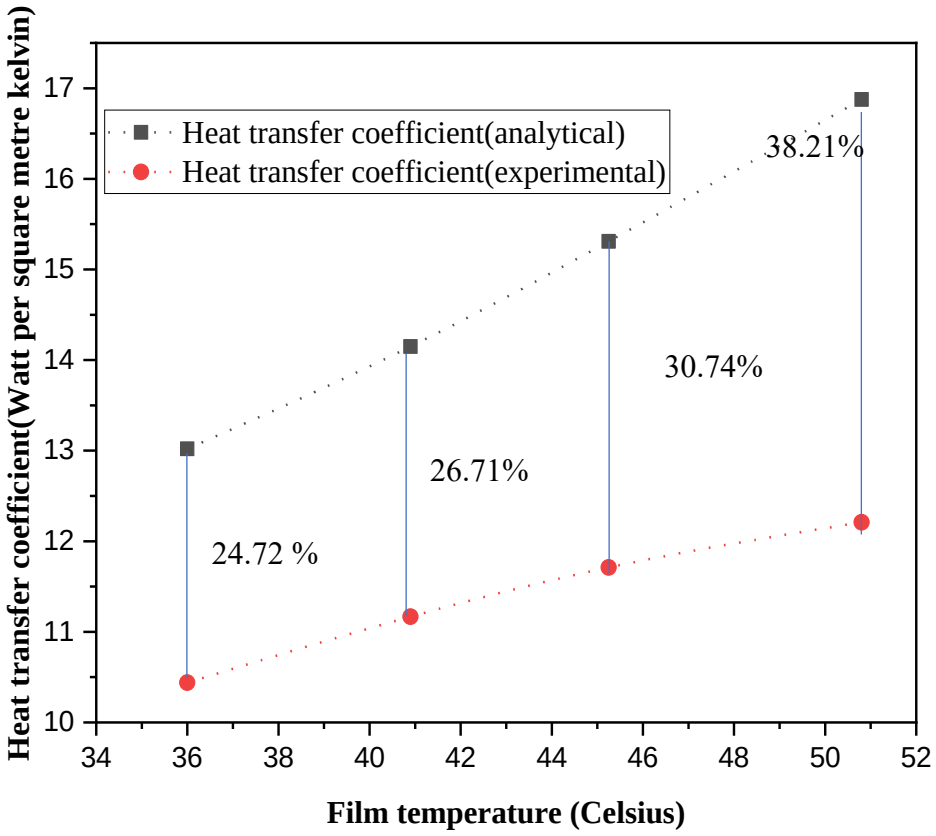

Fig. 5.11 Variation of heat transfer coefficient analytical vs experimental(Aluminium plugs under natural convection)

In the case of finned heat pipes under natural convection, the variation between heat transfer coefficient analytical and heat transfer coefficient experimental with film temperature is shown in Fig.5.12.

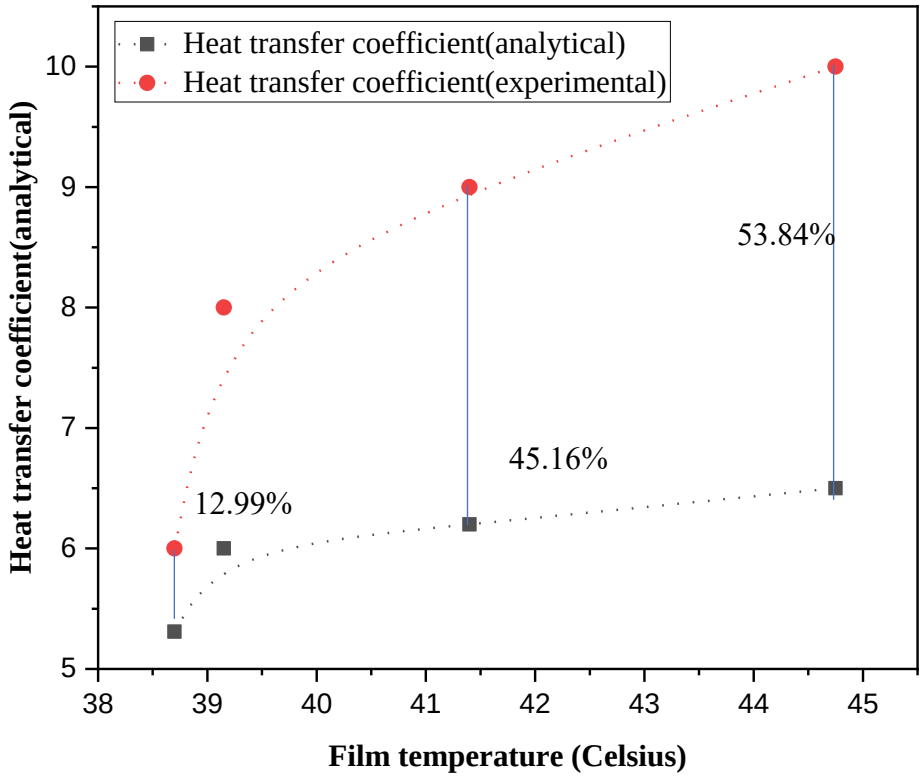

Fig. 5.12: Variation of heat transfer coefficient analytical vs experimental(Finned heat pipes)

In the case of finned aluminum rods under natural convection, the variation between heat transfer coefficient analytical and heat transfer coefficient experimental with film temperature is shown in Fig.5.13

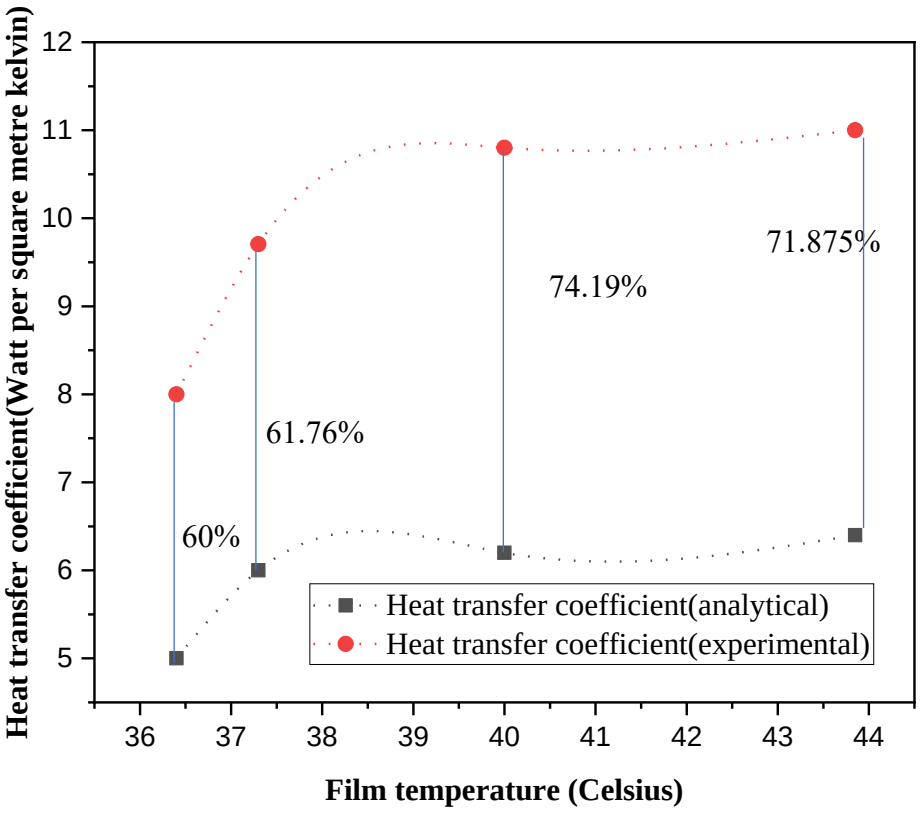

Fig. 5.13: Variation of heat transfer coefficient analytical vs experimental(Finned aluminum rods)

In the case of finned heat pipes under forced convection with heat input (Q) kept constant and velocity being varied condition, the variation between heat transfer coefficient analytical and heat transfer coefficient experimental with Reynold number is shown in Fig. 5.14.

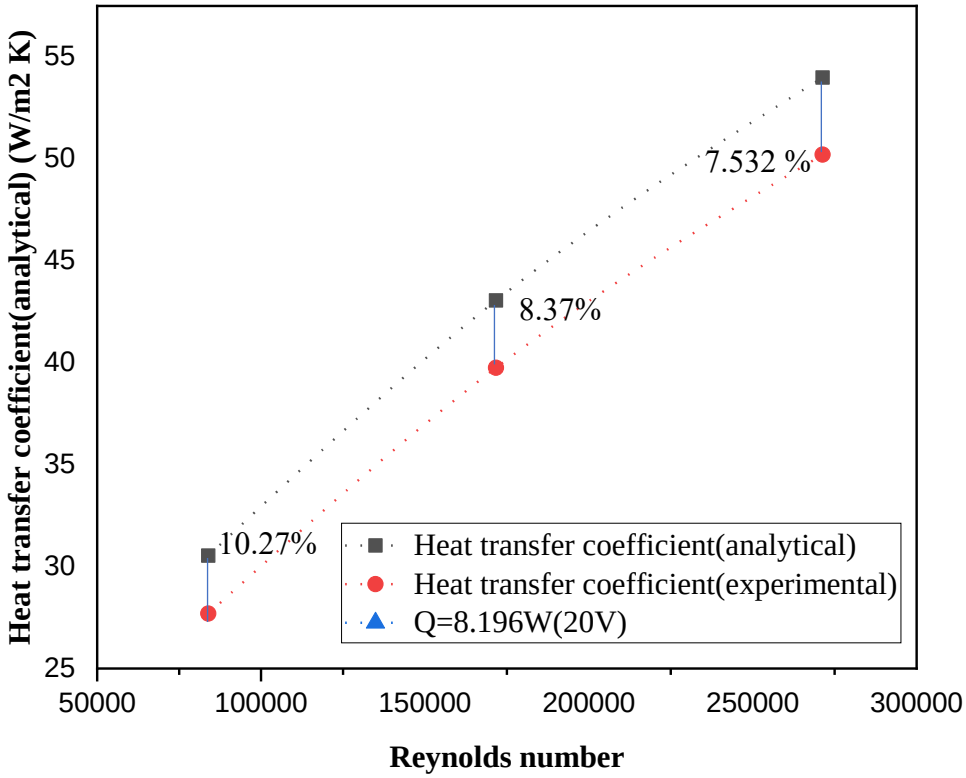

Fig. 5.14: Variation of heat transfer coefficient analytical vs experimental in forced convection(Finned heat pipes)

In the case of aluminum plugs under forced convection with heat input (Q) kept constant and velocity being varied condition, the variation between heat transfer coefficient analytical and heat transfer coefficient experimental with Reynold number is shown in Fig. 5.15.

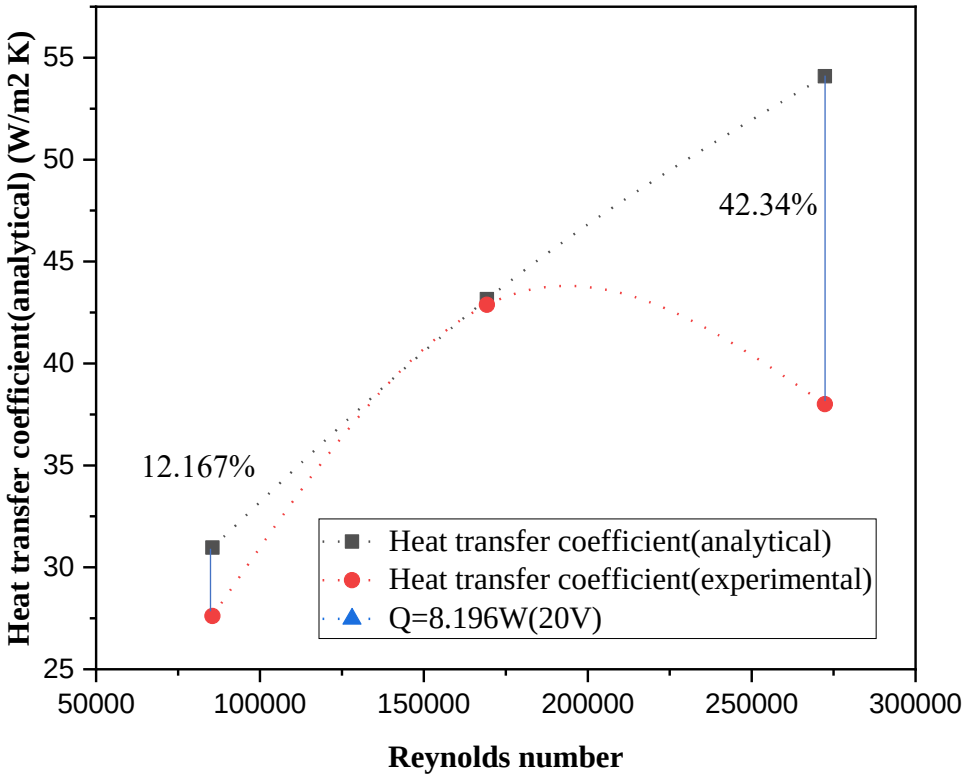

Fig. 5.15: Variation of heat transfer coefficient analytical vs experimental in forced convection(Aluminium plugs)

In the case of finned aluminum rods, under forced convection with heat input (Q) kept constant and velocity being varied condition, the variation between heat transfer coefficient analytical and heat transfer coefficient experimental with Reynold number is shown in Fig. 5.16.

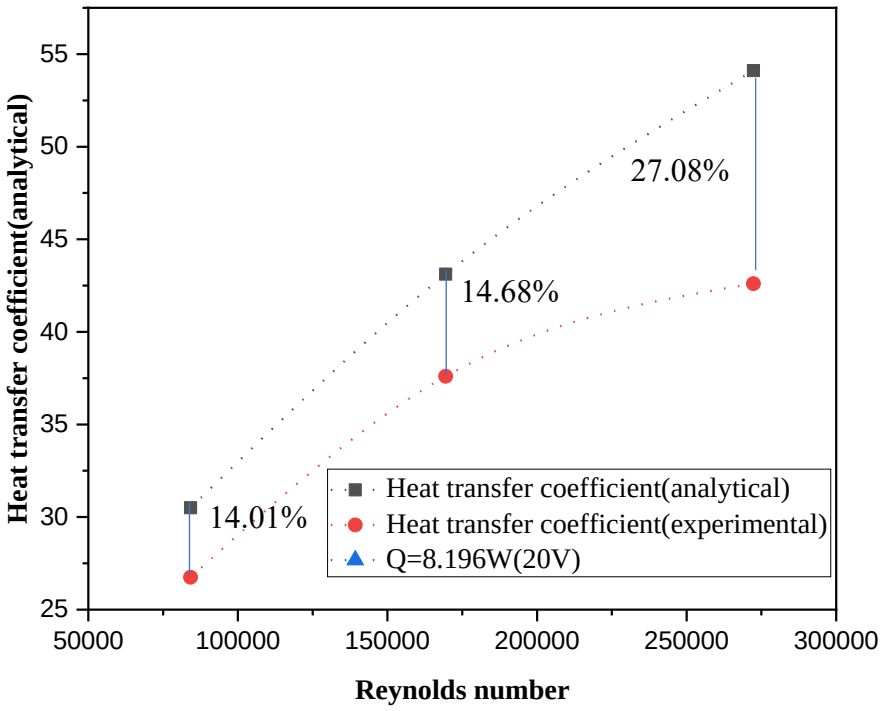

Fig. 5.16: **Variation of heat transfer coefficient analytical vs experimental in forced convection (Finned aluminum rods)**

CONCLUSION

1. In the case of natural convection, the least variation between heat transfer coefficient analytical and heat transfer coefficient experimental is observed in the case of aluminum plugs.

2. In the case of forced convection, the least variation between heat transfer coefficient analytical and heat transfer coefficient experimental is shown in the case of finned heat pipes.

3. In the case of natural convection maximum surface temperature was observed in the case of aluminum plugs.

4. In the case of forced convection, the maximum surface temperature was observed in the case of finned heat pipes.

FUTURE SCOPE

1. The testing of a different material of heat pipes can be done and performance can be determined based on the heat transfer coefficient.

2. The behavior of heat pipes made up can be analyzed under free and forced convection conditions.

References

[1] Maldonado, J.M., de Gracia, A. and Cabeza, L.F., 2020. A systematic review on the use of heat pipes in latent heat thermal energy storage tanks. *Journal of Energy Storage*, *32*, p.101733.

[2] Long, Z.Q. and Zhang, P., 2013. Experimental investigation of the heat transfer characteristics of a helium cryogenic thermosyphon. *Cryogenics*, *57*, pp.95-103.

[3] Jouhara, H., Chauhan, A., Nannou, T., Almahmoud, S., Delpech, B. and Wrobel, L.C., 2017. Heat pipe based systems-Advances and applications. *Energy*, *128*, pp.729-754.

[4] Qu, J., Wu, H.Y. and Cheng, P., 2010. Thermal performance of an oscillating heat pipe with Al2O3–water nanofluids. *International Communications in Heat and Mass Transfer*, *37*(2), pp.111-115.

[5] Peyghambarzadeh, S.M., Shahpouri, S., Aslanzadeh, N. and Rahimnejad, M., 2013. Thermal performance of different working fluids in a dual diameter circular heat pipe. *Ain Shams Engineering Journal*, *4*(4), pp.855-861.

[6] Adiguzel, N. and Irgatoglu, P.,2017. Investigation of The Effect of Nanofluids on Heat Transfer Performance of Heat Pipes. *Karamanoğlu Mehmetbey Üniversitesi Mühendislik ve Doğa Bilimleri Dergisi*, *3*(1), pp.44-73.

[7] Christodoulides, P., Agathokleous, R., Aresti, L., Kalogirou, S.A., Tassou, S.A. and Florides, G.A., 2022. Waste heat recovery technologies were revisited with emphasis on new solutions, including heat pipes, and case studies. *Energies*, *15*(1), p.384.

[8] Ji, Y., Ma, H., Su, F. and Wang, G., 2011. Particle size effect on heat transfer performance in an oscillating heat pipe. *Experimental Thermal and Fluid Science*, *35*(4), pp.724-727.

[9] Pachghare, P.R., 2013. Effect of Inclination Angle on the Thermal Performance of Closed Loop Pulsating Heat Pipe. *Int. J. Innov. Res. Sci. Technol*, *3*, pp.60-64.

[10] Nookaraju, B.C., Rao, P.K. and Nagasarada, S., 2015. Experimental and numerical analysis of thermal performance in heat pipes. *Procedia Engineering*, *127*, pp.800-808.

[11] Chirag, Dave, Dandale, P., Shrivastava, K., Dhaygude, D., Rahangdale, K., and Nilesh, M.O.R.E., 2021. A review on pulsating heat pipes: Latest research, applications and future scope. *Journal of Thermal Engineering*, *7*(3), pp.387-408.

[12] Karthikeyan, V.K., Ramachandran, K., Pillai, B.C. and Solomon, A.B., 2014. Effect of nanofluids on the thermal performance of closed-loop pulsating heat pipe. *Experimental Thermal and Fluid Science*, *54*, pp.171-178.

[13] Faghri, A., 2014. Heat pipes: review, opportunities, and challenges. *Frontiers in Heat Pipes (FHP)*, *5*(1).

[14] Vasiliev, L.L., 2005. Heat pipes in modern heat exchangers. *Applied thermal engineering*, *25*(1), pp.1-19.

[15] Pingale, A.D., Patil, C.M., and Marathe, P.B., 2017. Experimental investigation of thermosyphon for different parameters. *IOSR J. Mech. Civ. Eng*, *14*(01), pp.76-85.

[16] Teng, T.P., Hsu, H.G., Mo, H.E. and Chen, C.C., 2010. Thermal efficiency of heat pipe with alumina nanofluid. *Journal of alloys and compounds*, *504*, pp.S380-S384.

[17] Shafahi, M., Bianco, V., Vafai, K. and Manca, O., 2010. Thermal performance of flat-shaped heat pipes using nanofluids. *International journal of heat and mass transfer*, *53*(7-8), pp.1438-1445.

[18] Pachghare, P.R., 2013. Effect of Inclination Angle on the Thermal Performance of Closed Loop Pulsating Heat Pipe. *Int. J. Innov. Res. Sci. Technol*, *3*, pp.60-64.

[19] Goshayeshi, H.R., Safaei, M.R., Goodarzi, M. and Dahari, M., 2016. Particle size and type effects on heat transfer enhancement of Ferro-nanofluids in a pulsating heat pipe. *Powder Technology*, *301*, pp.1218-1226.

[20] Ahmad, H.H., 2012. Heat Transfer Characteristics in a Heat Pipe Using Water-Hydrocarbon Mixture as a Working Fluid.(An Experimental Study. *Al-Rafidain Engineering Journal (AREJ)*, *20*(3), pp.128-137.

[21] Jouhara, H., Anastasov, V. and Khamis, I., 2009. Potential of heat pipe technology in nuclear seawater desalination. *Desalination*, *249*(3), pp.1055-1061.

[22] Srimuang, W. and Amatachaya, P., 2012. A review of the applications of heat pipe heat exchangers for heat recovery. *Renewable and Sustainable Energy Reviews*, *16*(6), pp.4303-4315.

[23] Chan, C.W., Siqueiros, E., Ling-Chin, J., Royapoor, M. and Roskilly, A.P., 2015. Heat utilization technologies: A critical review of heat pipes. *Renewable and Sustainable Energy Reviews*, *50*, pp.615-627.

[24] Bai, L., Zhang, L., Lin, G., He, J., and Wen, D., 2015. Development of cryogenic loop heat pipes: A review and comparative analysis. *Applied Thermal Engineering*, *89*, pp.180-191.

[25] Gupta, M., Singh, V., Kumar, R., and Said, Z., 2017. A review on thermophysical properties of nanofluids and heat transfer applications. *Renewable and Sustainable Energy Reviews*, *74*, pp.638-670.

[26] Sureshkumar, R., Mohideen, S.T. and Nethaji, N., 2013. Heat transfer characteristics of nanofluids in heat pipes: a review. *Renewable and Sustainable Energy Reviews*, *20*, pp.397-410.

[27] Bolozdynya, A.I., Dmitrenko, V.V., Efremenko, Y.V., Khromov, A.V., Shafigullin, R.R. Shakirov, A.V., Sosnovtsev, V.V., Tolstukhin, I.A., Uteshev, Z.M. and Vlasik, K.F., 2015. The two-phase closed tubular cryogenic thermosyphon. *International Journal of Heat and Mass Transfer*, *80*, pp.159-162.

[28] Faghri, A., 2012. Review and advances in heat pipe science and technology. *Journal of heat transfer*, *134*(12).

[29] Sukchana, T. and Pratinthong, N., 2016. A two-phase closed thermosyphon with an adiabatic section using a flexible hose and R-134a filling. *Experimental Thermal and Fluid Science*, *77*, pp.317-326.

[30] Das, S.K., Choi, S.U. and Patel, H.E., 2006. Heat transfer in nanofluids—a review. *Heat transfer engineering*, *27*(10), pp.3-19.

[31] Xuan, Y. and Li, Q., 2003. Investigation of convective heat transfer and flow features of nanofluids. *J. Heat transfer*, *125*(1), pp.151-155.

[32] Tsai, C.Y., Chien, H.T., Ding, P.P., Chan, B., Luh, T.Y. and Chen, P.H., 2004. Effect of structural character of gold nanoparticles in nanofluid on heat pipe thermal performance. *Materials Letters*, *58*(9), pp.1461-1465.

[33] Sanitjai, S. and Goldstein, R.J., 2004. Forced convection heat transfer from a circular cylinder in crossflow to air and liquids. *International journal of heat and mass transfer*, *47*(22), pp.4795-4805.

[34] Bharti, R.P., Chhabra, R.P. and Eswaran, V., 2007. Steady forced convection heat transfer from a heated circular cylinder to power-law fluids. *International Journal of Heat and Mass Transfer*, *50*(5-6), pp.977-990.

[35] Xi N, Bai ML, Xu Z, Yang HW, Li H, Sun ZJ, 2006. Experimental and numerical studies on an integrated heat sink using heat pipes. J Eng Thermophys, 27(5):868–70.

[36] Naphon, P., Assadamongkol, P. and Borirak, T., 2008. Experimental investigation of titanium nanofluids on the heat pipe thermal efficiency. *International communications in heat and mass transfer*, *35*(10), pp.1316-1319.

[37] Chernysheva M, Maydanik Y., 2009. Heat and mass transfer in the evaporator of the loop heat pipe. J Thermophys Heat Transfer, 23:725–31.

[38] Lips, S., Sartre, V., Lefevre, F., Khandekar, S. and Bonjour, J., 2016. Overview of heat pipe studies during the period 2010−2015. *Interfacial Phenomena and Heat Transfer*, *4*(1).

[39] Aghvami, M. and Faghri, A., 2011. Analysis of flat heat pipes with various heating and cooling configurations. *Applied Thermal Engineering*, *31*(14-15), pp.2645-2655.

[40] Cao, Y., 2010, "Miniature High -Temperature Rotating Heat Pipes and their Applications in Gas Turbine Cooling," Frontiers in Heat Pipes (FHP), 1, 023002.

[41] Dobson, R. T., 2005, "An Open Oscillatory Heat Pipe Water Pump," Applied Thermal Engineering, 25(4), 603 -621.

[42] Do, K.H., Kim, S.J. and Garimella, S.V., 2008. A mathematical model for analyzing the thermal characteristics of a flat micro heat pipe with a grooved wick. *International Journal of Heat and Mass Transfer*, *51*(19-20), pp.4637-4650.

[43] Faghri, A. and Guo, Z., 2008. Integration of heat pipe into fuel cell technology. *Heat Transfer Engineering*, *29*(3), pp.232-238

[44] Jouhara, H. and Robinson, A.J., 2009. An experimental study of small-diameter wickless heat pipes operating in the temperature range 200 C to 450 C. *Heat Transfer Engineering*, *30*(13), pp.1041-1048.

[45] Kempers, R., Robinson, A.J., Ewing, D. and Ching, C.Y., 2008. Characterization of evaporator and condenser thermal resistances of a screen mesh wicked heat pipe. *International Journal of Heat and Mass Transfer*, *51*(25-26), pp.6039-6046.

[46] Ma, H.B., Wilson, C., Borgmeyer, B., Park, K., Yu, Q., Choi, S.U.S. and Tirumala, M., 2006. Effect of nanofluid on the heat transport capability in an oscillating heat pipe. *Applied Physics Letters*, *88*(14), p.143116.

[47] Saha, N., Das, P.K. and Sharma, P.K., 2014. Influence of process variables on the hydrodynamics and performance of a single loop pulsating heat pipe. *International Journal of Heat and Mass Transfer*, *74*, pp.238-250.

[48] L.G. Asirvatham, R. Nimmagadda, and S., 2013.Wongwises, "Heat transfer performance of screen mesh wick heat pipes using silver–water nanofluid," International Journal of Heat and Mass Transfer, vol. 60, pp. 201–209.

[49] Z. Xue and W. Qu, 2014. "Experimental study on the effect of inclination angles to ammonia pulsating heat pipe," Chinese Journal of Aeronautics, vol. 27, no. 5, pp. 1122–1127.

Ouriginal

Document Information

Analyzed document	Shubham ME Thesis.pdf (D142400005)
Submitted	7/25/2022 12:04:00 PM
Submitted by	
Submitter email	sayan.sadhu@thapar.edu
Similarity	16.5%
Analysis address	sayan.sadhu.thapar@analysis.urkund.com

Sources included in the report

W	URL: https://digitalcommons.mtu.edu/cgi/viewcontent.cgi?article=1460&context=etdr Fetched: 10/1/2019 8:39:45 AM	2
SA	**Anna University, Chennai / 20117201034-TS.pdf** Document 20117201034-TS.pdf (D46474868) Submitted by: adldirresearch@gmail.com Receiver: adldirresearch.annauniv@analysis.urkund.com	6
SA	**Parul University / 120370721006_Padhiyar Mehulkumar S Dissertation report.pdf** Document 120370721006_Padhiyar Mehulkumar S Dissertation report.pdf (D106451587) Submitted by: prashant.raj@paruluniversity.ac.in Receiver: prashant.raj.pau@analysis.urkund.com	1
SA	**Thapar Institute Of Engineering And Technology / thesis 3 plag.docx** Document thesis 3 plag.docx (D111582931) Submitted by: ananda@thapar.edu Receiver: ananda1.thapar@analysis.urkund.com	17
W	URL: https://dokumen.pub/download/heat-pipes-theory-design-and-applications-5nbsped-0750667540-9780750667548-9780080464770.html Fetched: 12/29/2020 3:17:34 AM	4
SA	**PSG College of Technology / Heat Pipe - Combined.docx** Document Heat Pipe - Combined.docx (D112797165) Submitted by: babu.mech@psgtech.ac.in Receiver: babu.mech.psgcot@analysis.urkund.com	4
W	URL: https://citeseerx.ist.psu.edu/viewdoc/download?doi=10.1.1.666.4760&rep=rep1&type=pdf Fetched: 7/25/2022 12:05:02 PM	1
SA	**National Institute Of Technology, Tiruchirapalli / HARIPRASANTH P PAPER.docx** Document HARIPRASANTH P PAPER.docx (D98739377) Submitted by: 411120003@nitt.edu Receiver: 411120003.nitt@analysis.urkund.com	3
W	URL: https://www.intechopen.com/chapters/67976 Fetched: 9/18/2021 12:33:36 PM	3

Ouriginal

W	URL: https://www.diva-portal.org/smash/get/diva2:1077524/FULLTEXT01.pdf Fetched: 2/25/2020 5:10:43 AM	4
W	URL: https://worldwidescience.org/topicpages/h/heat+pipe+operation.html Fetched: 7/3/2022 1:06:59 PM	1
W	URL: https://inpressco.com/wp-content/uploads/2015/08/Paper2210-213.pdf Fetched: 1/7/2022 8:10:59 AM	1
W	URL: https://inis.iaea.org/search/search.aspx?orig_q=RN:51008580 Fetched: 7/25/2022 12:04:45 PM	1
W	URL: https://www.sciencedirect.com/science/article/pii/S2352152X2031570X Fetched: 12/4/2020 2:20:32 PM	1
SA	**Anna University, Chennai / 10900331057-Renjith Singh-.pdf** Document 10900331057-Renjith Singh-.pdf (D19218134) Submitted by: manojvenkat90@gmail.com Receiver: adldirresearch.annauniv@analysis.urkund.com	2
SA	**Gujarat Technological University / Experimental investigation of closed loop oscillating heat pipe for combined effect of orientation and filling ratio using CuO Ethanol Nanofluid 120370721007.docx** Document Experimental investigation of closed loop oscillating heat pipe for combined effect of orientation and filling ratio using CuO Ethanol Nanofluid 120370721007.docx (D110611459) Submitted by: JIGNESH.R.VALA@GMAIL.COM Receiver: jignesh.r.vala.gtuni@analysis.urkund.com	5
SA	**Lunds universitet / Juan-Fu-Chapter 7 Heat pipes for aerospace application-V2-20160410.docx** Document Juan-Fu-Chapter 7 Heat pipes for aerospace application-V2-20160410.docx (D19220508) Submitted by: bengt.sunden@energy.lth.se Receiver: bengt.sunden.lu@analys.urkund.se	1
W	URL: https://link.springer.com/chapter/10.1007/978-3-319-29841-2_4 Fetched: 6/11/2020 4:56:08 PM	1
W	URL: https://www.semanticscholar.org/paper/The-Heat-Pipe-Eastman/c7f246fe8ec08b33f3a842840420097ead35a0ad Fetched: 7/25/2022 12:05:05 PM	1

Entire Document

1 STUDY OF PERFORMANCE OF DIFFERENT TYPES OF HEAT PIPES

80% **MATCHING BLOCK 1/59** W

A Thesis Submitted in Partial Fulfillment of Requirements for the Degree of Master of Engineering in Thermal Engineering